Transient and Steady-State Performance of A Liquid-to-Air Membrane Energy Exchanger (LAMEE)

A Thesis Submitted to the College of

Graduate Studies and Research

In Partial Fulfillment of the Requirements

For the Degree of Master of Science

In the Department of Mechanical Engineering

University of Saskatchewan

Saskatoon

By

Ramin Namvar

Permission to Use

In presenting this thesis in partial fulfillment of the requirements for a Postgraduate degree from the University of Saskatchewan, I agree that the Libraries of this University may make it freely available for inspection. I further agree that permission for copying of this thesis in any manner, in whole or in part, for scholarly purposes may be granted by the professor or professors who supervised my thesis work or, in their absence, by the Head of the Department or the Dean of the College in which my thesis work was done. It is understood that any copying or publication or use of this thesis or parts thereof for financial gain shall not be allowed without my written permission. It is also understood that due recognition shall be given to me and to the University of Saskatchewan in any scholarly use which may be made of any material in my thesis.

Requests for permission to copy or to make other use of material in this thesis in whole or part should be addressed to:

Head of the Department of Mechanical Engineering

University of Saskatchewan

Saskatoon, Saskatchewan (S7N 5A9)

ABSTRACT

The main objective of this thesis is to investigate the transient response and steady-state performance of a counter-cross flow liquid-to-air membrane energy exchanger (LAMEE). The LAMEE is constructed from several semi-permeable membranes which separate the air and liquid streams. In addition to heat transfer, moisture transfer occurs between the air and liquid streams since the membranes are permeable to water vapor. The LAMEE performance is assessed experimentally and the results are used to verify a numerical model. The verified numerical model is also used to extrapolate the transient and steady-state performance parameters to other test conditions.

The transient response of the LAMEE is important since there are times when the LAMEE operates under transient conditions due to daily start-up or changing operating conditions such as flow rates, temperatures or humidities. The transient response of the LAMEE is investigated experimentally and numerically. The number of heat transfer units (NTU), and the ratio of solution and air heat capacity rates (Cr*) are two important parameters that affect the LAMEE performance. The results show that the transient sensible, latent and total effectivenesses increases with time after a step change in the conditions of the inlet liquid desiccant. The experimental and numerical transient effectiveness values and trends are compared for different NTU and Cr* values under summer and winter test conditions and the results show satisfactory agreement.

In addition to the transient effectiveness, the time constant of the LAMEE is assessed as an important transient parameter. The time constant represents the time it takes for the LAMEE to reach 63.2% of the steady-state conditions after a step change in

inlet conditions. The transient response of the outdoor air temperature and humidity ratio are normalized and used to determine the sensible and latent time constants. It is found that time constant depends on NTU, Cr* and thermal mass capacity of the LAMEE. The experimental and numerical results show that time constant increases as Cr* decreases or NTU increases. Furthermore, the verified numerical model is used to study the effect of outdoor air conditions on the LAMEE time constant. The numerical results reveal that the latent time constant is influenced by outdoor air conditions and the time constant decreases as H* increases, but the sensible time constant is almost constant for various outdoor air conditions. However, the outdoor air conditions affect the transient response of the LAMEE considerably since the total transient response of the LAMEE is closer to the latent transient response for the conditions studied.

The steady-state performance of the LAMEE is studied for different NTU and Cr* values under summer test conditions. The experimental data are compared to numerical and analytical results and acceptable agreement is achieved. It is found that the steady-state effectiveness of the LAMEE increases with NTU and Cr*. The maximum total effectiveness reaches 88% for NTU=10 and Cr*=6.3. The verified numerical model is also used to investigate the effect of outdoor air conditions on the steady-state sensible and latent effectiveness of the LAMEE. The sensible effectiveness is significantly influenced by outdoor air conditions variation while the latent effectiveness is only slightly influenced by these variations. The sensible effectiveness decreases as the operating condition factor (H*) increases, but the latent effectiveness increases with H*.

ACKNOWLEDGEMENTS

I would like to express my deep gratitude to my supervisors, Professor C. J. Simonson and Professor Emeritus R.W. Besant. Thank you for your guidance and encouragement throughout this research. Without your support, leadership, and friendship this work would not have been possible.

I would like to acknowledge financial assistance from the Department of Mechanical Engineering, the Natural Science and Engineering Research Council of Canada (NSERC) and Venmar CES, Saskatoon.

DEDICATION

I dedicate this thesis to my parents, my wife and my brother.

Thank you very much for your love and encouragement throughout my life.

TABLE OF CONTENTS

Page

LIST OF TABLES

Table **Page**

LIST OF FIGURES

Figure **Page**

NOMENCLATURE

Acronyms

AHRI	Air-Conditioning, Heating and Refrigeration Institute
ASHRAE	American Society of Heating, Refrigerating and Air-Conditioning Engineers
HVAC	Heating, Ventilation and Air-Conditioning
LAMEE	Liquid-to-Air Membrane Energy Exchanger
RAMEE	Run-Around Membrane Energy Exchanger
RTD	Resistance Temperature Detector

English Symbols

A	surface area (m^2)
AAD	average absolute difference
b	channel width (m)
B	bias error
C	solution concentration
C_p	specific heat capacity (J/kg K)
C_d	discharge coefficient
C_{air}	heat capacity rate of air (W/K)
C_{sol}	heat capacity rate of solution (W/K)
Cr*	ratio of heat capacity rates (solution/air)
d	diameter of orifice plate (m)
D	inside pipe diameter (m)
E	modulus of elasticity
ER	energy recovery device
g	gravitational constant (m/s^2)

Gr	Grashof number
h	heat transfer coefficient (W/m^2K)
h_{fg}	heat of vaporization (J/Kg)
H	enthalpy (J/kg)
H*	operating factor
J	mass flux (kg/m^2s)
LPP	liquid penetration pressure
$\dot{m}$	mass flow rate (kg/s)
m*	mass flow rate ratio
M	mass (kg)
N	number of points
NTU	number of heat transfer units
NTU_m	number of mass transfer units
P	pressure (Pa)
Re	Reynolds number
Ri	Richardson number
RMSE	root mean square error
S	precision error
t	time (min)
t_1, t_2	first and second time constants (min)
t_{ex}	exchanger time delay
t^*	student's t value
T	temperature (˚C)
U	overall heat transfer coefficient (W/m^2K)
U_0	flow velocity (m/s)

U_m	overall mass transfer coefficient (kg/m^2s)
VDR	vapor diffusion resistance
W	humidity ratio (g/kg)
X	mass fraction (mass of water/ mass of salt)
x_1, x_2	dimensionless weighting factors

Greek Symbols

ε	effectiveness
Δ	difference in quantities
ρ	density (kg/m^3)
β	diameter ratio of orifice plate (m/m)
τ	single time constant (min)
γ	constant coefficient (NTU/NTU_m)
λ	constant coefficient (Cr/m^*)
η	fraction of the phase change energy absorbed by the solution
δ	gap thickness
ν	kinematic viscosity (m^2/s)

Subscript

air	air
ex	exchanger
exp	experimental
f	final
in	inlet
i	initial
L	latent
max	maximum

min	minimum
mem	membrane
num	numerical
out	outlet
S	sensible
salt	salt
sol	solution
ss	steady-state
T	total

CHAPTER 1

INTRODUCTION

1.1 Liquid-to-Air Membrane Energy Exchanger (LAMEE)

A liquid-to-air membrane energy exchanger (LAMEE) is a device used to transfer both sensible and latent energy between air and liquid flows. The LAMEE is constructed from semi-permeable membranes that are permeable to water vapor, but impermeable to liquid water. This characteristic is the main property of the LAMEE compared to heat exchangers which use metal plates between fluids and only are capable of sensible energy transfer.

The main application of LAMEEs is in energy recovery ventilators (ERV), which transfer energy between the supply and exhaust air streams of a heating, ventilation and air conditioning (HVAC) system. ERVs help to reduce the capital cost and energy consumption of HVAC systems while meeting the desired ventilation requires improving the indoor air quality (IAQ). For instance, a run-around membrane energy exchanger (RAMEE), which consists of two (one in each of the supply and exhaust air streams) LAMEEs coupled by a liquid desiccant loop, can reduce the energy consumption of a building by more than 50% (Rasouli et al. 2010a and 2010b). In addition to the RAMEE, another HVAC system that uses LAMEEs was designed and investigated by Bergero and Chiari (2010) and called “hybrid AC system”. The RAMEE and hybrid AC system are able to achieve significant energy savings. The LAMEE is the

main component of systems and the performance of these systems are significantly influenced by the LAMEE design and performance.

Several design parameters and operating conditions affect LAMEE performance. The steady-state performance of LAMEEs has been studied in literature and there are numerous analytical, numerical and experimental research in this area. Although LAMEEs are designed to operate in steady-state conditions in HVAC systems, there are times when the LAMEE will operate under transient conditions due to initial start-up of the HVAC system or quick changes in operating conditions. As a result, it is necessary to characterize the transient response of LAMEEs in order for effective control and to evaluate the impact of the LAMEE on other components in the HVAC system during the transient period.

1.2 Transient Response

Although the transient response of energy exchangers that transfer both heat and moisture has not been studied extensively, several analytical and experimental works on the transient response of heat exchangers have been carried out. The transient behavior of heat exchangers often occurs during initial start-up or shut down and it is necessary to predict the transient response of heat exchangers for effective control. Most of the research in this area studies the transient response of heat exchangers to a step change in inlet temperatures or flow rates.

Shah (1981) studied the transient response of heat exchangers with one-dimensional flow fields, and presented available solutions for the transient response of counter-flow and cross-flow heat exchangers to step changes in inlet temperatures and/or flow rates. These solutions were limited to specific conditions and only presented the

outlet temperature response. The transient response of a cross-flow heat exchanger to a step change in the hot fluid inlet temperature was also studied by Spiga and Spiga (1988, 1992). The two-dimensional transient temperature distributions in both fluids and wall were determined analytically using the Laplace transform method, considering a finite wall thermal capacity. The impact of the governing parameters (number of transfer units, capacity ratios, and heat transfer resistance ratio) on the dimensionless temperatures (or effectiveness) was studied.

The transient behavior of a liquid-to-air fin and tube heat exchanger was studied numerically for step changes in water and air inlet temperatures (Vaisi et al. 2011). The results showed that the outlet temperature of the fluid that was subjected to a step change reaches steady-state conditions faster than the other fluid outlet temperature. The time constant of the system was defined when the outlet temperature reaches 99% of the step change and was used to represent the time that the fluid reaches steady-state. Vaisi et al. (2011) found that the time constant was not affected by the amplitude of step change in inlet temperature of hot or cold fluids. Ataer et al. (1995) developed three different numerical approaches to investigate the transient performance of a cross-flow finned-tube liquid/gas heat exchanger for a step change in the hot fluid inlet temperature. The three approaches had different assumptions concerning the heat capacitance of the fins, wall and fluids. The transient dimensionless outlet temperatures of the hot and cold fluids were presented for a step change in the hot fluid inlet temperature. These numerical results were compared to experimental data. Afterward, an approximate analytical approach was used to predict the transient response of the heat exchanger for a step change in the hot fluid inlet temperature (Ataer, 2004). This analytical solution

characterized the dynamic behavior of the heat exchanger with a time constant, a delay time and a gain.

The transient response of a heat exchanger was investigated after a step change in the fluid inlet temperature and/or mass flow rate (Yin and Jensen, 2003). The transient temperature distribution of the single-phase fluid and wall were calculated using an integral method. This analytical solution was compared to other numerical solutions and there was a good agreement over a wide range of operating conditions. The results are applicable to various configurations of heat exchangers (such as counter-flow, parallel flow and cross-flow) since one of the fluids has a constant temperature and the flow arrangement becomes irrelevant in the analytical solution.

Most analytical and numerical models for the transient response of plate heat exchangers assume a uniform flow distribution; however, in reality the flow could be mal-distributed. A numerical model developed to predict the transient performance of plate heat exchangers after a step flow variation, considering the port to channel flow mal-distribution (Dwivedi and Das, 2007). In reality the flow is not equally distributed between channels and the flow velocity varies from channel to channel. The flow mal-distribution was found to affect the transient response of the heat exchanger considerably. The numerical model was validated against the experimental results. Results were presented for a wide range of designs (NTU) and operating (heat capacity rate ratio) parameters. Srihari (2005) developed an analytical model for the dynamic behavior of a plate heat exchanger, considering the separate effects of flow mal-distribution from channel to channel and fluid backmixing within a channel. The governing equations were solved by using the Laplace transform method and the results

showed that the heat exchanger effectiveness reduces with mal-distribution, while the mal-distribution from channel to channel has a greater impact on the heat exchanger performance than fluid axial dispersion within a channel. It was found that the influence of mal-distribution depends on the axial dispersive Peclet number and the number of plates, but it is almost independent of NTU and the heat capacity rate ratio. The effect of mal-distribution on the transient response of plate heat exchangers was also investigated numerically and experimentally by Srihari and Das (2008). The results revealed that flow mal-distribution affects the transient parameters such as initial delay, response time and time constants.

The transient response of a run-around membrane energy exchanger (RAMEE) system was investigated experimentally and numerically by Seyed-Ahmadi et al. (2008a and 2008b) and Erb et al. (2009a). The transient sensible, latent and total effectiveness were presented for different design parameters and operating conditions. Since, the transient response of the RAMEE depends on the transient behavior of the LAMEE, it is important to investigate the transient response of a single liquid-to-air membrane energy exchanger (LAMEE), which is the purpose of this M.Sc. research.

1.3 Steady-State Performance

In addition to the transient response of the LAMEE, the steady-state performance of the LAMEE is important as it is expected the LAMEE operates more hours under steady-state conditions. A heat and mass transfer model for an air-to-air enthalpy exchanger with a porous membrane core was developed and used to calculate the temperature and humidity in steady-state conditions (Zhang and Jiang, 1999). The fundamental dimensionless groups were derived and validated with experimental data

(Niu and Zhang, 2001). The impact of the membrane properties and operating conditions on the sensible, latent and enthalpy effectiveness were studied. The results revealed that the membrane material and operating conditions affect the latent and enthalpy effectiveness considerably, while the sensible effectiveness mainly depends on the number of transfer units (NTU).

Another mathematical model was developed to study coupled heat and moisture transfer in a membrane-based enthalpy exchanger (Ming and Su, 2010a). The effect of membrane properties (such as the moisture diffusivity, thermal conductivity, thickness and membrane spacing) on the exchanger steady-state performance was investigated. The results showed that the effect of membrane thermal conductivity on all effectivenesses is negligible since less than 10% of the exchanger total thermal resistance is due to the membrane thermal resistance, while the membrane moisture resistance accounts for 65-90% of the total moisture resistance. They subsequently found that the sensible effectiveness is not significantly influenced by the membrane moisture diffusivity, but the latent effectiveness is strongly dependant on the moisture diffusivity of the membrane. The effects of the membrane thickness and channel height on the exchanger performance were also investigated and it was suggested to use a thin membrane and a moderate channel height in order to obtain better performance (Ming and Su, 2010b).

Zhang (2011) developed an analytical solution to heat and mass transfer in hollow fiber LAMEEs. The governing equations of heat and mass transfer between the liquid and air flows were solved and the analytical solution could estimate the air and desiccant solution outlet conditions and sensible and latent effectiveness at steady-state.

The model was validated by steady-state experiments. Parametric analysis showed that the total number of transfer units for heat and mass transfer have dominant impact on the sensible and latent effectiveness. Also, a numerical model was used to investigate the hollow fiber LAMEE (Zhang et al., 2012). The local and mean Nusselt and Sherwood numbers for air and liquid desiccant were obtained and validated by experimental data. The results showed that the real boundary conditions are neither uniform temperature nor uniform heat flux. Recently, Huang (2012) used the real boundary conditions on the membrane surface which were obtained numerically to investigate the heat and moisture transfer in membrane-formed parallel-plates channels.

The steady-state performance of liquid-to-air membrane energy exchangers was investigated experimentally and numerically (Chiari, 2000; Bergero et al., 2001a and 2001b). The heat and moisture transfer between the air and liquid (water or LiCl solution) were studied for flat-plate and hollow-fiber cross-flow membrane energy exchangers. The effects of various parameters on the vapor mass flux through the membrane were studied and the results showed that the latent effectiveness increases as the air flow rate decreases or the liquid flow rate increases.

Furthermore, energy recovery systems consisting two LAMEEs on the supply and exhaust air streams were investigated in several studies under steady-state conditions (Bergero and Chiari, 2005; Mahmud et al., 2010; Erb et al., 2009a; Hemingson et al., 2011a). The effects of air and liquid desiccant flow rates, exchange surface of the LAMEEs and outdoor air conditions on the steady-state performance of energy recovery systems were investigated. These systems showed significant energy saving under steady-state conditions for both heating and cooling. Therefore, LAMEEs

have a significant potential in HVAC systems provided their transient performance is satisfactory.

1.4 Thesis Objectives and Overview

As mentioned previously, the transient response of the LAMEE has not been characterized extensively in literature. In this thesis, the transient heat and moisture transfer characteristics in the LAMEE for different design parameters and operating conditions will be investigated. Experimental data will be used to verify a numerical model that predicts the transient response and steady-state performance of the LAMEE for various air and liquid desiccant mass flow rates under summer and winter test conditions. The verified numerical model will be used to investigate the impact of outdoor air conditions on the transient and steady-state performance of the LAMEE. The main objectives of this M.Sc. thesis are listed below:

1. Determine (experimentally) the transient behavior and steady-state performance of a counter-cross flow LAMEE for various design and operating parameters.
2. Compare the experimental results with a numerical data and verify the model for the heat and moisture transfer characteristics of the LAMEE
3. Use the verified numerical model to identify the effect of outdoor air conditions on the transient response and steady-state performance of the LAMEE

These objectives are addressed in two research manuscripts as listed below:

1. **R. Namvar**, D. Pyra, G. Ge, C.J. Simonson, R.W. Besant, Transient characteristics of a liquid-to-air membrane energy exchanger (LAMEE) experimental data with

correlations, accepted by International Journal of Heat and Mass Transfer (June 2012)

2. **R. Namvar**, C.J. Simonson, R.W. Besant, Transient heat and moisture transfer characteristics of a liquid-to-air membrane energy exchanger (LAMEE) model verification and extrapolation, submitted to International Journal of Heat and Mass Transfer (August 2012)

Manuscript #1 and #2 are presented in chapters 2 and 3, respectively. Chapter 2 describes the LAMEE structure and experimental set-up, and presents experimental data on the transient and steady-state performance of the LAMEE **(objective 1)**.

The experimental results are compared to numerical data in chapter 3 and the numerical model is verified **(objective 2)**. The verified model is used to investigate the effect of initial conditions on the transient performance of the LAMEE and quantify the uncertainty in experimental data due to the uncertainty in the initial conditions. The numerical model is also used to show the impact of outdoor air conditions on the LAMEE performance **(objective 3)**.

In chapter 4, the main conclusions of this thesis are summarized and recommendations for future LAMEE research are also presented.

CHAPTER 2

EXPERIMENTAL DATA AND CORRELATIONS

2.1 Overview of Chapter 2

The transient and steady-state performance of the LAMEE is investigated experimentally in this chapter, which contains manuscript #1 (Transient characteristics of a liquid-to-air membrane energy exchanger (LAMEE) experimental data with correlations). In the manuscript, the LAMEE structure and experimental tests apparatus are presented and mass and energy balance are performed for the LAMEE. The transient response of the LAMEE is studied for different air and liquid desiccant mass flow rates under summer and winter test conditions. The transient outlet temperature and humidity ratio are used to characterize the transient behavior of the LAMEE and to determine the heat and moisture transfer time constants. Finally, the experimental steady-state sensible, latent and total effectiveness data are presented experimentally and compared with analytical results. The experimental data presented in this chapter will be used in chapter 3 to verify the LAMEE numerical model.

Three students contributed to the completion of this research. Dave Pyra began this research by conducting some tests for different air and desiccant mass flow rates. Gaoming Ge used the analytical solution of Zhang (2011) to generate the analytical effectiveness data presented in Figure 2.9. My contribution in this research was to: (a)

develop and complete the experimental test plan, (b) determine the uncertainty of experimental data and (c) post-process the results and write the paper.

Manuscript #1: Transient Characteristics of a Liquid-to-Air Membrane Energy Exchanger (LAMEE) Experimental Data with Correlations

Ramin Namvar, Dave Pyra, Gaoming Ge, Carey J. Simonson[*]*, Robert W. Besant*

2.2 Abstract

In this paper, the transient and steady-state performance of a liquid to air membrane energy exchanger (LAMEE) is investigated experimentally. The transient sensible, latent and total effectiveness are each presented for particular air and desiccant mass flow rate for both summer and winter supply air test conditions. After a step change in inlet conditions the effectiveness increases with time. Also, the transient effectiveness is assessed for various air and desiccant mass flow rates under summer test conditions and the LAMEE's time constant is investigated as an important variable that depends primarily on the thermal capacity of the exchanger and liquid content. The calculated effectiveness shows considerable dependency on the air and desiccant mass flow rate. Finally, steady-state results reveal that as the desiccant mass flow rate increases or air mass flow rate decreases, the effectiveness increases.

2.3 Introduction

Energy consumption is important topic for the economy and environment. Buildings consume 40% of the world primary energy and account for about one third of the emissions of the green house gases (GHG) in the world (Perez-Lombard et al., 1998). More than 50% of the building energy consumption is used for heating, ventilation and air-conditioning (HVAC) systems (ANSI/ASHRAE Std. 90.1, 2007). Since people spend more than 90% of their time inside the buildings (ANSI/ASHRAE Std. 55, 2004), indoor air quality (IAQ) and occupant comfort are important

considerations. In order to maintain a healthy and comfortable indoor air conditions, outside fresh air must be supplied to the buildings for ventilation; however, without energy recovery this ventilation air increases the energy consumption. As a result, researchers, designers, and manufacturers are working on new strategies to achieve a good balance between good indoor air quality (IAQ) and the energy consumption in buildings. Using air-to-air energy recovery (ER) systems is one of these new strategies.

Energy recovery systems recover energy from the exhaust air to condition the supply air. This process decreases energy consumption and peak rates of energy input, so the size or capacity of the heating and cooling equipment may be decreased (Erb et al., 2009a). ER systems are able to transfer moisture as well as heat, and they can improve the indoor air quality (IAQ). The run-around membrane energy exchanger (RAMEE) system is a novel air-to-air energy recovery system. The RAMEE is compromised of two remote liquid-to-air membrane energy exchangers (LAMEEs) connected by a pumped salt solution to transfer both sensible and latent energy between the supply and exhaust air. The LAMEEs structure is similar to traditional air-to-air heat exchangers with metal plates, except porous membranes are used instead of metal heat exchange plates. These membranes are semi-permeable and able to transfer both heat and water vapor, but not liquid water or salt solution. These exchangers have a large exchanger surface areas per unit of volume, do not directly transfer contaminants such as bacteria or other particulate materials between air streams, and modest friction losses on both air and solution sides (Bergero and Chiari, 2005).

Several experimental and numerical studies have been done for a RAMEE system. For example, a cross-flow RAMEE system was modeled numerically by Fan et

al. (2006). This investigation showed that this type system could have an acceptable performance and its total effectiveness could reach up to 70%. A cross-flow prototype with Propore^{TM} membrane was constructed by Erb (2009b) and its steady-state and transient performance was assessed. The size of each LAMEE was 100 mm wide, 600 mm long and 400 mm high. The transient effectiveness of the RAMEE was assessed at NTU=11.3 for summer and winter test conditions at Cr*=15 and Cr*=22, respectively. The experimental and numerical results showed good agreement for sensible, latent and total effectiveness. The transient performance of the RAMEE system was very slow and it took over five hours to reach a quasi steady-state. Also, steady-state performance of the RAMEE was assessed only under summer test conditions for several different NTU and Cr* values, and its steady-state total effectiveness was only 43% (Erb et al., 2009a). The RAMEE showed higher effectiveness values for large values of Cr*; however, the effectiveness decreases at low Cr* values likely due to flow maldistribution and non-uniform contact between the liquid desiccant and membrane (Erb, 2009b).

It was shown by Vali (2009) that the flow configuration in the LAMEE affects the performance of the RAMEE system. The results indicated that a counter-cross flow LAMEE with small entrance ratio and exchanger aspect ratio could perform better than a cross-flow LAMEE with the same surface area. A new counter-cross flow configuration prototype of dimensions 200×1800×86 mm was constructed and tested by Mahmud (2009). The steady-state performance of this system was investigated in this research and it achieved the maximum total effectiveness of 55% (i.e. above the minimum of 50% required by ASHRAE standard 90.1 (ANSI/ASHRAE, 2007) under AHRI standard test conditions (Mahmud et al., 2010). Also, effect of air and desiccant mass flow rates

on the steady-state effectiveness was studied and the results showed that the effectiveness of the system increases when the air flow rate is decreased or desiccant flow rate is increased.

Another experimental investigation was conducted for steady-state air humidification using a single cross-flow LAMEE (Chiari, 2000). The dimensions of the LAMEE used in this experiment was 450×90×50 mm which is smaller compared to Erb or Mahmud's LAMEE. The air flow rates in the tests ranged from 10 to 80 m^3/h (2.78 to 22.22 L/s), while the 19°C water flow rate was from 0.005 to 0.015 kg/s. The results confirmed Mahmud's results and revealed that the LAMEE's latent effectiveness increases as the air flow rate decreases or the water flow rate increases. However, in this research just latent effectiveness was investigated, and there was no data taken to calculate the sensible or total effectiveness. Also, air humidification and dehumidification through this LAMEE was analyzed in another research paper by Bergero and Chairi (2001). In this research humidification with water and dehumidification with LiCl were investigated. In both cases, the inlet air was at 24-25˚C and 50% RH and the flow rate was 30 to 80 m^3/h (8.33 to 22.22 L/s). The latent effectiveness of the LAMEE was found to be between 60% and 80%, and effectiveness decreased as the air mass flow rate increased.

The transient response of the LAMEE is important because the exchanger should be able to react quickly to rapid weather changes and, more repeatedly initial start-up changes following a period when the LAMEE is off overnight or during a weekend. If the LAMEE does not react quickly during the system start up, the LAMEE may not transfer enough heat and moisture such that the desired outlet conditions will not be

achieved which will put extra load on the other equipment in the HVAC system (Erb, 2009b). Although many exchangers have small transient time constants so their performance can be considered as steady-state in HVAC applications (Abe et al., 2006a), LAMEEs have time constants that are about 10 times larger. These larger time constants are due to the large thermal and moisture capacities of LAMEEs and the coupled heat and moisture transfers that occur in LAMEEs. For example, Erb et al. (2009a) found that, for a RAMEE with two LAMEEs, it may take over five hours to reach steady-state. For LAMEEs used in systems other than a RAMEE the time delays for step changes can be very different.

Most of previous research on this area has investigated steady-state performance of the LAMEE, but there is not sufficient data about the transient performance of the system. The main purpose of this research is to investigate transient performance of a counter-cross single liquid-to-air membrane energy exchanger (LAMEE). Sensible, latent and total effectiveness values are assessed during a transient step change in inlet conditions for different air and desiccant liquid mass flow rates. Finally, steady-state performance of the system is studied for different mass flow rates.

2.4 The LAMEE

2.4.1 LAMEE Structure

The LAMEE consists of many rectangular flow panels where each panel consists of two semi-permeable membranes, two outer screens, one inner screen, and air spacers (Beriault, 2010). Each liquid flow channel in a panel is constrained by two membranes through which heat and moisture can be transferred between the liquid and air channels.

In this experiment, a counter cross LAMEE is investigated. As it is shown in Figure 2.1, the inlet and outlet of desiccant channel, and the air channel are perpendicular to each other, but the desiccant and air flows are mostly counter-flow. Ten panels are combined with two external Aluminum frames to make a LAMEE which is 1.218 m long, 0.305 m high and 0.1 m wide. Inside the exchanger, spacers are used to support air and desiccant channels. In addition, spacers hold two outer screen pieces against the membrane to reduce the deflections of the membrane into air stream (Beriault, 2010). The properties of the LAMEE are shown in Table 2.1.

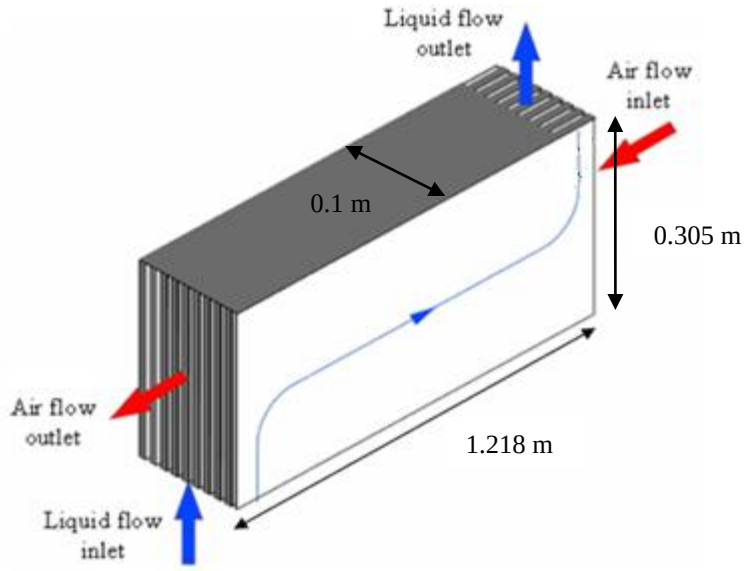

Figure 2.1 A counter-cross liquid-to-air membrane energy exchanger (LAMEE) showing one liquid streamline (Vali, 2009)

Table 2.1 The LAMEE and membrane dimensions and properties

LAMEE Properties	
Exchanger length (m)	1.218
Exchanger width (m)	0.305
Number of panels	10
Aspect ratio (L/W)	4
Air gap thickness (mm)	6.35
Solution gap thickness (mm)	3.17
Solution inlet length (m)	0.066
Specific heat capacity (J/kg˚K)	1.16
Total mass (kg)	28
Membrane type	ePTFE-AY Tech
Mass resistance of membrane (s/m)	97
Membrane thermal conductivity (W/m)	0.334
Membrane thickness (mm)	0.54

The run-around membrane energy exchanger (RAMEE) system shown in Figure 2.2 is an air-to-air energy recovery system which is comprised of one liquid-to-air membrane energy exchanger (LAMEE) in each of the supply and exhaust air flow channels coupled by a pumped liquid desiccant loop. The LAMEEs are coupled by a liquid desiccant loop, which transfers the heat and moisture between the two exchangers. The desiccant solution gains or loses heat and moisture from/to the air streams through the semipermeable membrane inside each LAMEE.

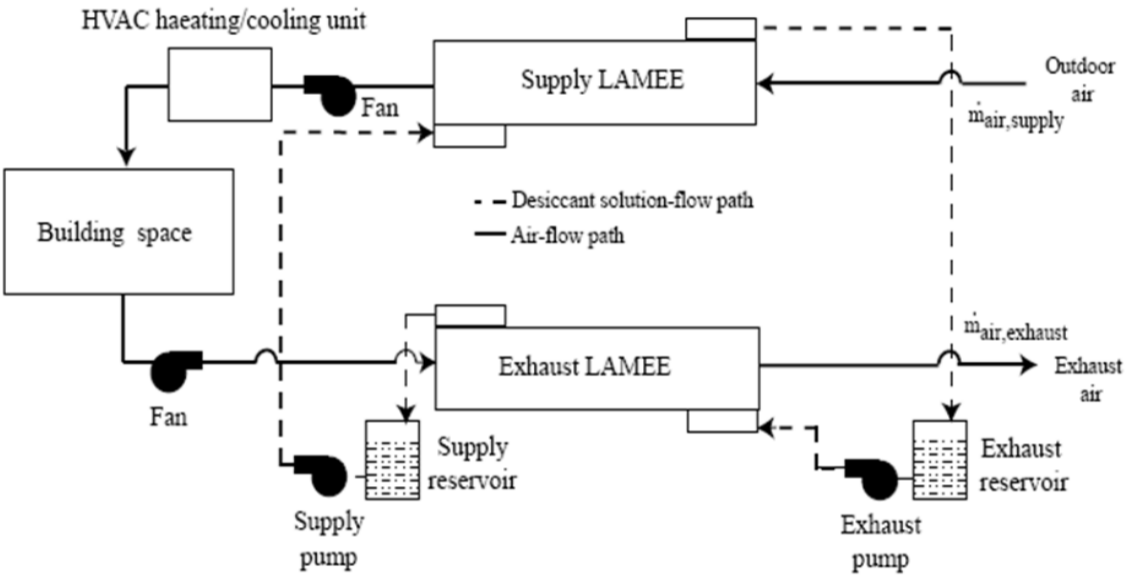

Figure 2.2 Schematic of a run-around membrane energy exchanger (RAMEE) system (Mahmud, 2009)

2.4.2 Membrane Properties

The main difference between the LAMEE and heat exchangers is its use of semi-permeable membranes. The performance of the LAMEE heavily depends on membranes' properties. There are several polyethylene and polypropylene semi-permeable membranes which could be used as a membrane in the LAMEE, but finally the AY Tech. ePTFE Laminate was selected as the membrane due to its small vapor diffusion resistance (VDR), high liquid penetration pressure (LPP), and good modulus of elasticity (E) (Beriault, 2010).

As mentioned, the moisture transfer is the main priority of the LAMEE compared to heat exchangers. VDR is an important parameter which is inversely proportional to the membrane rate of vapor transfer. The lower VDR, the faster moisture transfer. As a result, the latent effectiveness of the LAMEE improves if a membrane with a lower VDR is used. This is important as the total effectiveness in previous prototypes was limited by their vapor transfer rate. The Permatran-W® test apparatus is

used to measure the water vapor transmission rate through the membrane and VDR is calculated using these data. The results show that the AY Tech. membrane's VDR is 97 ± 11 s/m (Beriault, 2010).

The LPP indicates the water pressure at which liquid water will pass through a membrane. As the operating pressure of the LAMEE is below 5 psi (34 kPa) (Mahmud, 2009), the liquid desiccant should not leak into the air streams because AY Tech. ePTFE Laminate LPP is more than 12 psi (82 kPa). Moreover, the membrane elasticity should be considered as well. The higher the modulus of elasticity, the less deflection in the membrane, and it leads to less flow misdistribution in flow channels and higher LAMEE effectiveness. The modulus of elasticity for the AY Tech. ePTFE Laminate is 387 ± 32 MPa which is higher compared to other membranes such as Propore™ (Beriault, 2010).

2.4.3 Desiccant Solution

There are many desiccant solutions available and suitable for the LAMEE system such as lithium bromide, lithium chloride, calcium chloride, and magnesium chloride. All of these solutions are able to transfer heat and water vapor, but the main consideration for choosing a desiccant is crystallization. It is important the LAMEE system operates without any desiccant crystallization because salt crystals attached to the membrane surfaces reduce the moisture transfer between air and desiccant and may cause a flow mal-distribution so the LAMEE's performance will be reduced (Afshin et al., 2010). In addition, desiccant channel blockage, membrane fouling and improper desiccant pumping are other consequences of the crystallization (Charles and Johnson, 2008). LiCl-water solution can be used in almost all climates without any crystallization while $MgCl_2$ may crystallize in very dry outdoor conditions (Afshin et al., 2010).

However, magnesium chloride ($MgCl_2$) solution is chosen due to its availability and lower cost in this research. $MgCl_2$ concentration during experiments of this research was found to be less than saturation concentration (35.9%) for each test, which means there is not any crystallization risk for $MgCl_2$. The solution concentration is defined by equation (2.1):

$$C = \frac{\text{mass of salt}}{\text{mass of salt+mass of water}} \tag{2.1}$$

The rate of water vapor that desiccant solution absorbs or desorbs from/to the air flow in the LAMEE depends on the vapor pressure difference between the air and desiccant liquid flows. The desiccant vapor pressure is related to the desiccant's concentration and temperature (ASHRAE, 2005). Larson et al. (2007) found that the relative humidity has very small effect on the properties of membrane so the increase in the moisture transfer is due to the increase in vapor pressure difference not a change in VDR. The humidity ratio of the air at equilibrium with the desiccant solution is determined using the correlations developed by Cisternas and Lam (1991).

2.4.4 Performance Evaluation

The main purpose of this research is investigating transient response of a counter-cross single liquid-to-air membrane energy exchanger (LAMEE) and evaluating its performance under various conditions. According to the ASHRAE Standard 84 (ANSI/ASHRAE, 2008), the most important parameter in ER systems is their effectiveness. As was shown, LAMEEs are the main components of the RAMEE system and the effectiveness of the whole system depends on the LAMEE's effectiveness. There are three types of energy transfer effectiveness (sensible ε_s, latent ε_l and total ε_t)

(ANSI/ASHRAE Std. 84, 2008). In this paper if effectiveness is used without a qualifier, then it refers to all three. As a result, the most important parameters in the LAMEE performance are its sensible, latent and total effectiveness. These parameters are equal to the ratio of the actual heat (sensible energy), moisture (latent energy) or total energy transfer rate divided by the maximum possible transfer rate of each of these energies. The following definitions of effectiveness appear somewhat different from standard definitions in the literature since the thermal capacity rate ratio for the tests presented in this paper is 1.0.

The sensible effectiveness shows the exchanger ability to transfer heat between the air stream and liquid desiccant and when the thermal capacity rate ratio is 1.0, it is defined as:

$$\varepsilon_{\mathrm{S}} = \frac{(T_{\mathrm{air,in}} - T_{\mathrm{air,out}})}{(T_{\mathrm{air,in}} - T_{\mathrm{sol,in}})} \tag{2.2}$$

The latent effectiveness indicates the exchanger ability to transfer moisture and phase change energy and it is developed for an energy capacity rate ratio of 1.0:

$$\varepsilon_{\mathrm{L}} = \frac{(W_{\mathrm{air,in}} - W_{\mathrm{air,out}})}{(W_{\mathrm{air,in}} - W_{\mathrm{sol,in}})} \tag{2.3}$$

The above two effectiveness ratios apply to the LAMEE when Cr* is greater than 1.0, which is the most common operating condition for the LAMEE.

The total energy or enthalpy effectiveness is related to both heat and moisture transfer and it is calculated from following equation (Simonson and Besant, 1999):

$$\varepsilon_T = \frac{\varepsilon_S + H^* \varepsilon_L}{(1 + H^*)} \tag{2.4}$$

where H^* is the operating factor and it depends on the air and desiccant solution inlet conditions (Simonson and Besant, 1999):

$$H^* = \frac{\Delta H_L}{\Delta H_S} = 2500 \frac{W_{air,in} - W_{sol,in}}{T_{air,in} - T_{sol,in}} \tag{2.5}$$

These equations assume no external heat losses/gains and also no condensation or frosting due to cold surface temperatures (Mahmud et al. 2010).

There are two independent operating variables which affect the system effectiveness such as air and desiccant mass flow rates. These dimensionless variables are the number of transfer units (NTU) and ratio of heat capacity rates (Cr*) which vary inversely proportional to the air mass flow rate when Cr*>1,

$$NTU = \frac{UA}{C_{\min}} \tag{2.6}$$

$$Cr^* = \frac{C_{Sol}}{C_{air}} = \frac{1}{Cr} \tag{2.7}$$

where U is the overall heat transfer coefficient (W/m^2K), A is the membrane area in the LAMEE system (m^2), C_{Sol} and C_{air} are the heat capacity of the desiccant solution and air, respectively, and C_{min} is the minimum value of C_{sol} and C_{air}.

The analytical solution for the effectiveness of a single counter flow heat exchanger at steady-state conditions is given by (Incropera and Dewitt, 2002):

$$\varepsilon_{S,Counter} = \frac{1 - \exp[-NTU(1 - Cr)]}{1 - Cr \exp[-NTU(1 - Cr)]} \tag{2.8}$$

Similarly, the steady-state latent effectiveness is calculated by equation (2.9) (Nasif et al., 2005):

$$\varepsilon_{L,Counter} = \frac{1 - \exp -[NTU_m(1 - m^*)]}{1 - (m^*) \exp[-NTU_m(1 - m^*)]} \tag{2.9}$$

where,

$$NTU_m = \frac{U_m A}{\dot{m}_{min}} \tag{2.10}$$

$$m^* = \frac{\dot{m}_{min}}{\dot{m}_{max}} = \frac{\dot{m}_{air}}{\dot{m}_{sol}} \tag{2.11}$$

In equation (2.10), U_m is the overall mass transfer coefficient and m_{min} is the minimum mass flow rate between the air and desiccant. It should be noted that, for the experimental data presented in this paper, there is a nearly constant relationship between NTU and NTU_m and also between Cr and m* which is:

$$NTU = \gamma NTU_m \tag{2.12}$$

$$Cr = \lambda m^* \tag{2.13}$$

where γ and λ are constant coefficients:

$$\gamma = \frac{U}{U_m Cp_{air}} \tag{2.14}$$

$$\lambda = \frac{Cp_{air}}{Cp_{sol}} \tag{2.15}$$

Another analytical solution for a counter hollow fiber membrane exchanger is developed by Zhang (2011) which predicts steady-state sensible and latent effectiveness. In this model air stream and desiccant solution flow are in a counter flow arrangement and the problem is solved in one-dimension. Heat and moisture losses through the shell to the surroundings and axial dispersion of heat and mass are negligible.

2.5 Experimental Set-up

2.5.1 Test Apparatus

Figure 2.3 contains a schematic of the experimental facility used to test the LAMEE. The test facility provides the property measurements for the inlet and outlet air and desiccant streams. The air is provided to the LAMEE from an environmental chamber and it leaves to the ambient air in the laboratory while the desiccant flows from supply reservoir to the exhaust one.

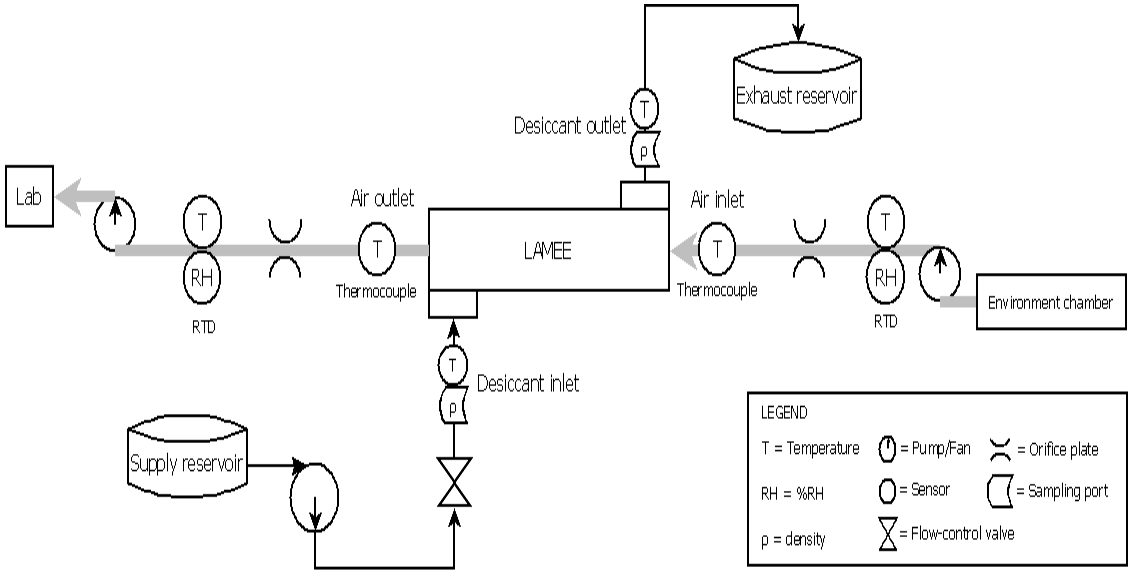

Figure 2.3 Schematic experimental set up

The outdoor air condition is provided by an environmental chamber. The range of temperature which the chamber can simulate is between -40˚C and 40˚C, and it provides up to 90% relative humidity (RH). The conditioned air inside the chamber is provided to the LAMEE as supply air and is emitted to the laboratory after passing through the LAMEE. Two variable speed 5 hp fans blow and vacuum the air before and after the LAMEE which reduces the pressure difference between the airstream and ambient pressure at the exchanger to nearly zero (Erb et al., 2009a). These fans are used to set the desired airflow rate by controlling the electrical power supplied to them. Before the LAMEE entrance, there is a honeycomb flow straighter which reduces the vortices in the airflow up stream of each orifice flow meter.

As soon as desired inlet air conditions are satisfied, the desiccant solution pump is turned on while the air flow fans are operating. The pump is a 62 W centrifugal pump for circulating the desiccant solution to a liquid flow rate between 0.38 and 5.68 liters per minute. During each test, the liquid desiccant's samples are taken to measure its properties and density. All ducts and tubes in both air and liquid loops are insulated to reduce the rate of heat loss or gain.

The data acquisition system for this experiment consists of a terminal block, signal conditioner and data acquisition board. The terminal block (model: NI SCXI 1303) takes data from all sensors (thermocouples, humidity sensors and pressure transducers) and transfers them to the signal conditioner. The main role of the signal conditioner (Model NI SCXI 1000) is synchronizing the timing of all the data with different signal types between the terminal blocks and data acquisition board (Mahmud, 2009). As these data are analogue, a data acquisition board (model: NI PCI 6251) is

required to convert these analog signals to digital signals before sending them to the computer. The computer gathers 100 data every 10 s at speed of 1 kHz and for each property its average is shown through a LabView program.

2.5.2 Uncertainty and Calibration

Figure 2.3 shows the schematic of the experimental set-up and positions of the instruments used to measure the air and desiccant properties to evaluate the performance of the LAMEE. For the air stream, its temperature, humidity and mass flow rate are measured. The air mass flow rate is measured by using orifice plates which are designed to satisfy ISO Standard 5167-1 (ISO, 1991). Orifice plate pressure drop is converted to the mass flow rate using equation (2.16):

$$\dot{m} = C_d \frac{\pi}{4} d^2 [\frac{2\rho(\Delta P)}{1-\beta^4}]^{1/2} \tag{2.16}$$

where the C_d is discharge coefficient of orifice plate, d is diameter of orifice plate (m), D is inside pipe diameter (m), ΔP is pressure drop across orifice plate (Pa), ρ is air density (kg/m^3) and β is d/D.

To measure the air stream temperature both thermocouple and resistance temperature device (RTD) are used. All temperature sensors were calibrated using a temperature simulator (DAVIS Instruments model 9107) with ±0.1°C accuracy. To reduce the uncertainty, three thermocouples are spaced along the height of exchanger inlet and outlet and the average temperature is recorded. In order to calculate the humidity ratio of the air (W_{air}), air temperature and its relative humidity (RH) are

measured by using a calibrated VAISALA humidity and temperature transmitter (Model: HMP233).

According to Figure 2.3 only the temperature and density of the desiccant are measured in this experiment. To prevent sensors errors due to salt solution contact shielded T-type thermocouples are used to measure the temperature. These thermocouples are larger and show less sensitivity and accuracy compared to air side ones. Density of the desiccant solution is measured by a density meter with 0.0001 g/cm^3 accuracy.

Although calibration reduces the bias uncertainty, B, of a sensor, the precision, S, exists for each steady-state measurement. The measured properties uncertainty consists of the precision and bias errors. According to the ASME PTC 19.1 (ASME, 1998) the overall uncertainty at 95% confidence interval is combination of these two errors and is calculated using:

$$U_{95} = \sqrt{B^2 + (tS)^2} \tag{2.17}$$

where B is bias error, S is precision error, and t is the Student-t value which depends on the number of measurements, N, for N>30, t=2. For calculated parameters, uncertainty is calculated by using the error propagation method (Figliola and Beasley, 2000). Their uncertainties depend on the uncertainties of the measured parameters and instruments. The precision, bias and overall uncertainty of each sensor are shown in Table 2.2.

Table 2.2 Measurement instruments uncertainties at 95% confidence interval

Measurement	Precision (S)	Bias (B)	$U_{95\%}$	Units
RTD-Air Temperature	0.024	0.2	0.21	˚K
Thermocouple Air-Temp	0.05	0.1	0.14	˚K
Thermocouple Desiccant-Temp	0.07	0.1	0.17	˚K
Air Humidity	0.3%	1.0%	1.2%	% RH
Desiccant Flow Rate	0.15	0.05	0.25	L/min

2.5.3 Mass and Energy Balances

It is necessary to perform the mass and energy balance for the LAMEE to verify that the systematic errors due to unaccounted heat or moisture transfer in the experiment are negligible. For a steady-state energy balance for fluid flow and if there are no external heat gains/losses, the following equation should be satisfied (ANSI/ASHRAE Std. 84, 2008):

$$\frac{\left|\dot{m}_{air,in}h_{air,in} - \dot{m}_{air,out}h_{air,out} + \dot{m}_{sol,in}h_{sol,in} - \dot{m}_{sol,out}h_{sol,out}\right|}{\dot{m}_{air,in}h_{air,in} + \dot{m}_{sol,in}h_{sol,in}} \leq 0.1 \qquad (2.18)$$

When calculating the mass and energy balance, it is assumed that inlet and outlet air mass flow rates are equal and that the mass flow rate of salt is constant in the LAMEE. After the first few minutes, for all the tests, the energy in balance (equation (2.18)) is less than 0.05 or 5% while its uncertainty varied from 4% to 9%. Since this energy balance equation is only for steady-state it does not include transient sensible

energy rate gain from or to the solid structural components of the exchanger. That is, the rate of sensible energy transfer within the solid structure during the transient heat and moisture tests is less than the convective energy exchange rate across the membrane surface area. As the water mass flow rate in the desiccant solution is up to two orders of magnitude higher than the water vapor mass flow rate in the air stream, dividing the vapor mass difference between inlet and outlet to the total inlet vapor mass results in values lower than 1% for the vapor mass imbalance. To account for this large difference twice the vapor mass of inlet air is used instead of total inlet vapor mass in denominator of following water flow rate mass balance equation:

$$\frac{\left|\dot{m}_{air,in}W_{air,in} - \dot{m}_{air,out}W_{air,out} + \dot{m}_{salt,in}X_{sol,in} - \dot{m}_{salt,out}X_{sol,out}\right|}{2\times\dot{m}_{air,in}W_{air,in}} \leq 0.1 \qquad (2.19)$$

The mass rate balance values for equation (2.19) are from 1% to 8% for all the tests. Also, the uncertainty in the calculated water vapor and energy balances in the LAMEE due to uncertainties in the measured properties and sensors uncertainty values varies from 2% to 9% for all tests. All these data are presented in Table 2.3, and both mass and energy balances are satisfied for all the experimental tests in the paper.

Table 2.3 Mass and energy balances and uncertainties for all experiments

NTU	Cr*	Mass Balance %	U_M %	Energy Balance %	U_E %
6	1.3	6.4	6.6	2.2	8.5
	3.9	7.3	2.8	1.2	5.7
	6.3	7.9	2	2.3	4.3
8	1.3	3.2	9.3	4.7	8.8
	3.9	6.8	3.4	0.6	5.6
	6.3	1.7	2.4	1.4	4.3
10	1.3	4.6	5.1	3.8	6.1
	3.9	1	4.2	0.2	5.8
	6.3	3.3	2.8	3.3	4.5

2.5.4 Test Conditions

In this research, inlet air conditions in all tests are determined according to AHRI standard 1060 (AHRI, 2005) which are shown in Table 2.4. Temperature and humidity of the inlet air should be as close as possible to the standard conditions; however, due to some practical limitations there is a difference between standard conditions and actual test conditions. For example, the winter supply air temperature is higher than AHRI standard due to humidity content in environment and saturated condition. For summer test conditions, the inlet conditions are close to the standard conditions, but they are slightly different from test to test and average values are presented in Table 2.4. The air inlet temperature varies from 34 to 35.3 ˚C and its humidity ratio range is from 24 to 27 g/kg.

Table 2.4 American Heating and Refrigeration Institute 1060-2005 standard test conditions and actual test conditions

		AHRI Condition	*Actual Test Condition*
Summer	Air Inlet Temperature	**35˚C**	**34.9˚C**
	Air Inlet Humidity Ratio	**17.5 g/kg**	**26 g/kg**
Winter	Air Inlet Temperature	**1.7˚C**	**7.8˚C**
	Air Inlet Humidity Ratio	**3.5 g/kg**	**3.1 g/kg**

The desiccant inlet temperature and concentration should be clarified. The main concern for the liquid desiccant condition is to avoid crystallization. That is, the desiccant concentration should be less than saturated concentration everywhere in the exchanger during each test. As the desiccant reservoir is in the laboratory, its inlet temperature varies from 23.4 to 25.9 ˚C for different tests and the average is 24.6˚C. The average humidity ratio and desiccant concentration are 12 g/kg and 30%, respectively.

2.6 Results and Discussions

The transient performance of the LAMEE is important during its start-up when the system is shut down. Also, if the outdoor conditions change rapidly, the LAMEE should be able to respond quickly to this condition. In this paper, step changes in the desiccant conditions are investigated as they play a more important role in the LAMEE performance compared to the changes in the air operating conditions which can be studied in future research. The transient inlet and outlet conditions of air and desiccant are presented for selected air and desiccant mass flow rates and for all other tests transient response is normalized to determine the LAMEE time constant for different air

and desiccant mass flow rates. Then, the transient effectiveness is discussed for one of the tests and finally the effect of air and desiccant mass flow rate on the steady-state effectiveness of the LAMEE is assessed.

2.6.1 Transient Data

First, the transient data for a specific test with constant air and desiccant mass flow rate are presented. The air inlet condition is close to AHRI standard summer test condition and desiccant inlet condition is T_{sol} = 24.4˚C and W_{sol} = 11 g/kg. Before starting the test, the exchanger is full of liquid desiccant and the airstream passes through the exchanger until it reaches as close as possible to the AHRI standard test conditions. Then, the desiccant solution pump is turned on and this is regarded as the start for each test (i.e., t=0). It almost takes 30 min for these selected air and liquid desiccant mass flow rates for the LAMEE to reach a steady-state condition. The transient inlet and outlet conditions of the air and desiccant are shown in Figure 2.4. As it is shown, the inlet conditions are almost constant during the test, but outlet conditions change until they reach to steady values. In Figure 2.4a, for the first two minutes of the test the air outlet temperature and for the first seven minutes of the test the desiccant outlet temperature are higher than 34˚C (maximum inlet temperature). This change is mainly a result of the air and desiccant initial conditions inside the LAMEE. As mentioned, before starting the test, the LAMEE is filled by a high concentration desiccant and as hot and humid air passes through it, the air is dehumidified, and this dehumidification releases water vapor phase change energy inside the LAMEE. As a result, the outlet temperatures are higher than maximum inlet temperature due to high rates of phase change.

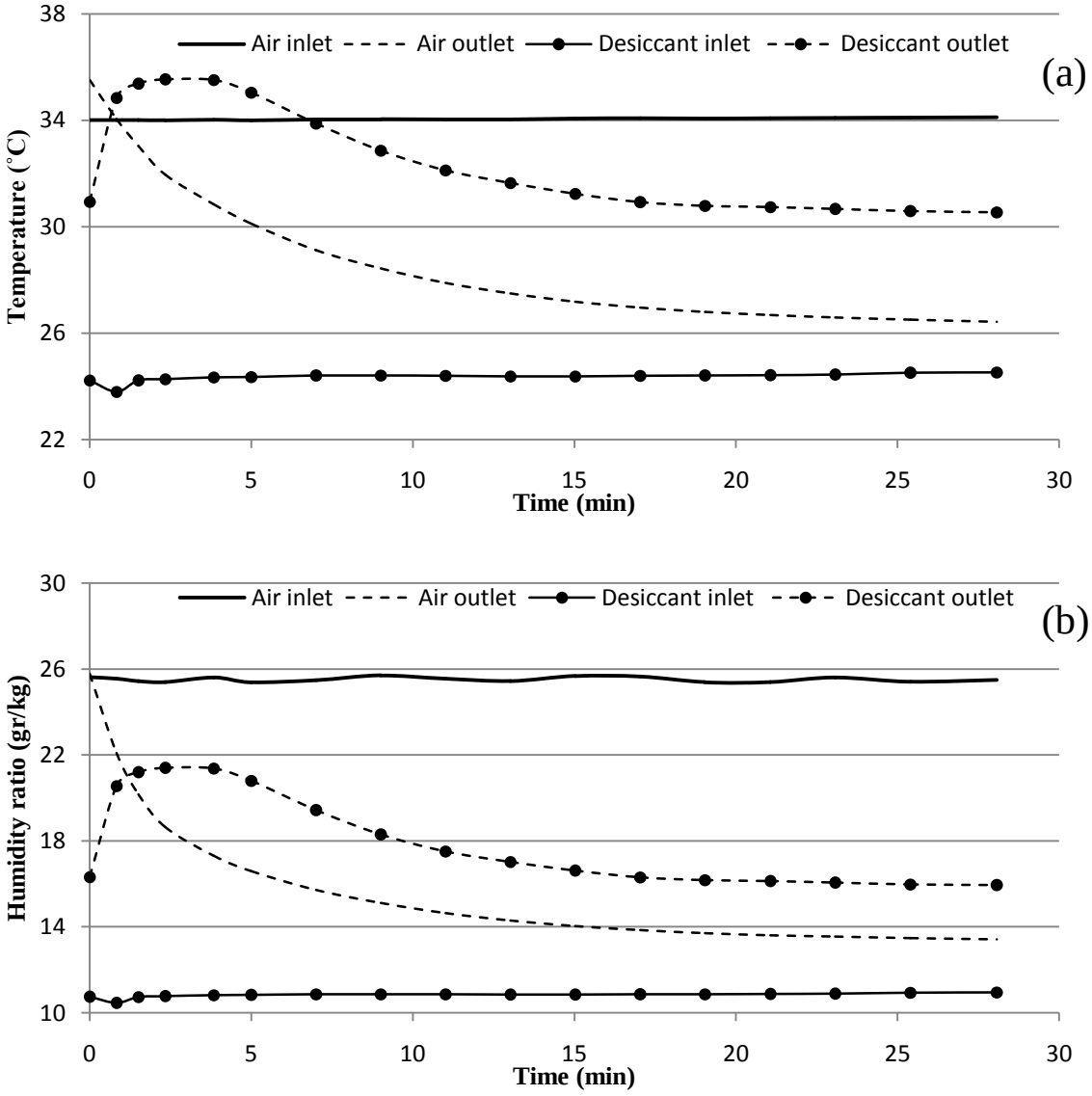

Figure 2.4 . Transient a) temperature and b) humidity of air and desiccant inlet and outlet for NTU = 8 and Cr* = 6.3

In order to characterize these transient responses and compare them for different tests, air outlet conditions are normalized. An exponential correlation with two dimensionless weighting constants and two time constants is fitted to the air outlet temperature and humidity ratio (Abe et al., 2006b):

$$\frac{\Delta\Phi}{\Delta\Phi_{\circ}} = X_1 e^{-t/t_1} + X_2 e^{-t/t_2} \tag{2.20}$$

where

$\Delta\Phi = |\Phi - \Phi_i|$ change in variable φ (temperature or humidity ratio) at any time, t, compared to the initial value (φ_i)

$\Delta\Phi_\circ = |\Phi_f - \Phi_i|$ maximum change in the variable from its initial value to the final value

t_1, t_2 the first and second time constants

The weighting constants satisfy the equation:

$$X_1+X_2 = 1, \quad X_1 \geq 0, \quad X_2 \geq 0 \tag{2.21}$$

For example, this correlation is fitted to the normalized air outlet temperature of the presented test in Figure 2.4a and the normalized values and curve fit are shown in Figure 2.5. There is a very good agreement between experimental data and correlations. The value of each coefficient, X_1, X_2, t_1, t_2, is determined by using MATLAB software for all tests with different air and desiccant mass flow rates. They are presented in Table 2.5 for both temperature and humidity ratio. The r^2 value in the table shows the quality curve fit for each.

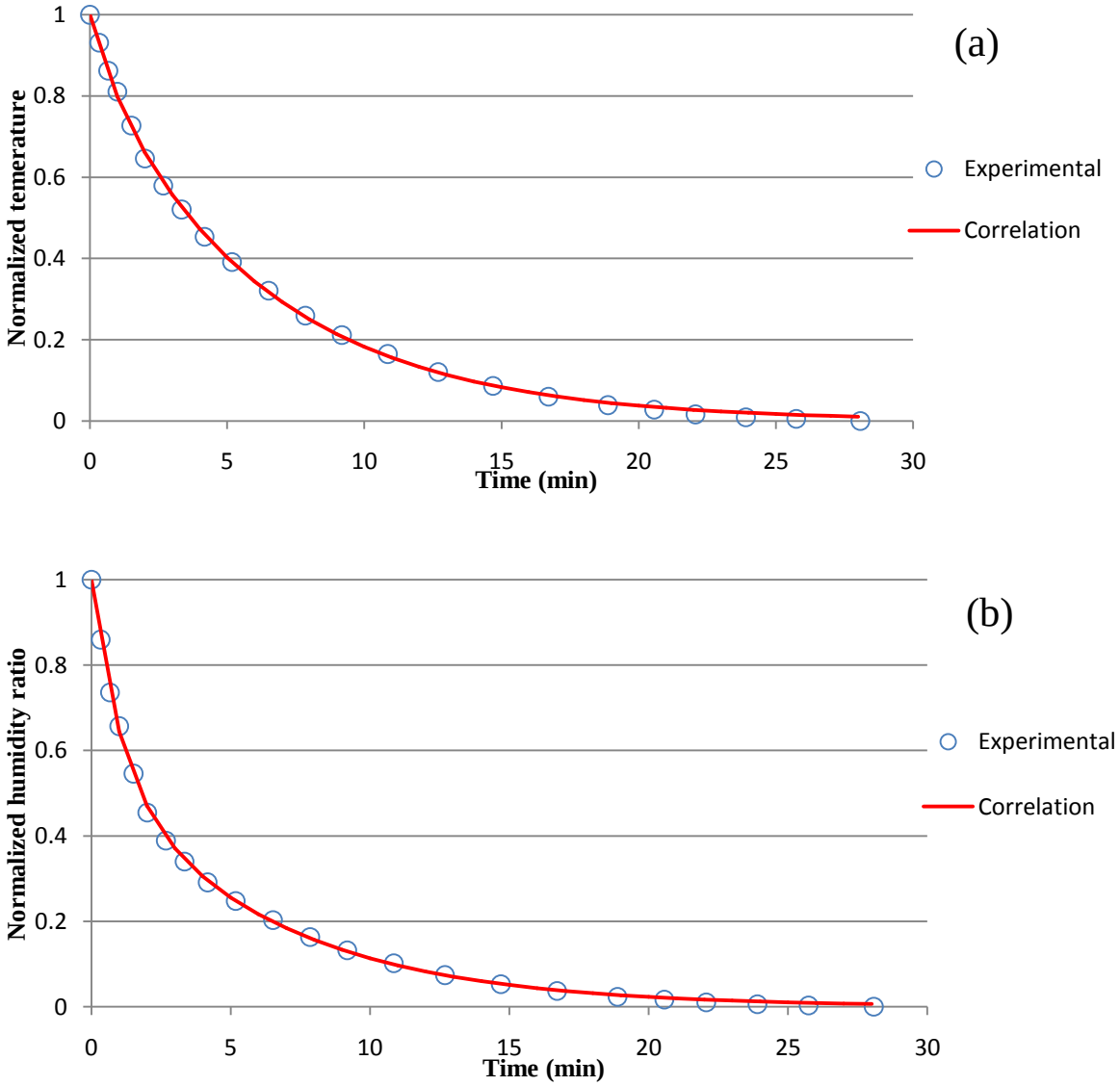

Figure 2.5 Air outlet Normalized a) temperature (X_1= 0.12, X_2= 0.88, t_1= 1, t_2= 6.3) and b) humidity ratio (X_1= 0.44, X_2= 0.56, t_1= 1, t_2= 6.3).

Table 2.5 Dimensionless weighting factors (x_1, x_2) and time constants (t_1, t_2) describing the transient air outlet conditions

NTU	Cr*	Air outlet temperature						
		T_i (˚C)	T_f (˚C)	χ_1	τ_1 (min)	χ_2	τ_2(min)	r^2
6	1.3	35.5	31.1	0.60	1.0	0.40	14.4	0.97
	3.9	36.2	28.5	0.03	2.6	0.97	6.9	0.95
	6.3	36.6	27.7	0.15	1.3	0.85	5.2	0.99
8	1.3	38.0	31.7	0.46	4.6	0.54	21.1	0.99
	3.9	38.3	28.6	0.17	1.6	0.83	10.1	0.99
	6.3	35.5	26.4	0.12	1.0	0.88	6.3	0.99
10	1.3	36.7	30.5	0.36	3.7	0.64	23.4	0.99
	3.9	38.8	26.0	0.20	3.4	0.80	13.4	0.99
	6.3	38.1	26.1	0.15	1.8	0.85	8.7	0.99
		Air outlet humidity ratio						
		W_i (g/kg)	W_f (g/kg)	χ_1	τ_1(min)	χ_2	τ_2(min)	r^2
6	1.3	26.3	20.6	0.58	2.2	0.42	12.4	0.96
	3.9	23.3	15.4	0.57	1.7	0.43	7.2	0.94
	6.3	25.2	14.3	0.56	1.0	0.44	5.2	0.99
8	1.3	27.5	19.6	0.58	2.4	0.42	21.0	0.99
	3.9	28.2	15.2	0.48	1.3	0.52	10.5	0.99
	6.3	25.8	13.4	0.44	1.0	0.56	6.3	0.99
10	1.3	26.9	18.2	0.54	2.8	0.46	22.5	0.99
	3.9	28.4	13.6	0.49	2.3	0.51	13.3	0.99
	6.3	28.2	12.5	0.51	1.5	0.49	8.8	0.99

As it can be seen in Table 2.5 the first time constant is less than second time constant for all tests. The first time constant is less than 5 min which correlates to the time it takes for the liquid desiccant to flow through the LAMEE for each test which is referred to as the desiccant transport time for the exchanger. The desiccant transport time depends on the desiccant mass flow rate or Cr* value, but it is less than 5 min for Cr* 1.3-6.3. Generally, the second time constant shows larger values of t_2 than t_1, and t_2 changes from 5 to 24 min. These high values appear to correlate with the LAMEE thermal mass capacity which delays the response of the LAMEE. Before starting each test, the LAMEE structure is in thermal equilibrium with the temperature of the

laboratory air, and it takes time for the temperature of the LAMEE structure to become in equilibrium with the air and desiccant flowing through the LAMEE. In addition to the transport time delay, the conduction heat rate exchange within the exchanger is greatest near time t=0. That is, the conduction heat transfer rate within the exchanger structural components is balanced by some of the changes in the conductive heat transfer rate inside the exchanger and this exchange rate is greatest at the beginning of each test. The time delay of the exchanger is calculated using equation (2.22) and its value is 25±3 min for the exchanger. The second time constant is of the order of this time delay and is related to the thermal mass capacity of the LAMEE. Moreover, with few exceptions, both t_1 and t_2 increases as Cr* decreases or NTU increases. In general, lower air or desiccant mass flow rates, the higher time constant values.

$$t_{ex} = \frac{M_{ex} C_{P,ex}}{h_{air} A_{ex}} \tag{2.22}$$

The transient response of the measurement sensors is included in the presented time constant values, as well as the LAMEE transient response and it causes an error in these values. According to Wang et al. (2006) if it is assumed the sensors respond instantaneously, time constant values will be changed by 10-20% for the energy wheel used (Wang et al., 2006). But, for the energy wheel, the first and second time constants are 3 s and 100-300 s respectively, and these values are much less than the time constants for the LAMEE. As a result, the sensor transient response impact on the time constants for the LAMEE will be negligible.

According to equation (2.20), two time constants are defined for the LAMEE. The first and second time constants are related to the desiccant transport time inside the LAMEE and thermal mass capacity of the LAMEE, respectively. It is instructive to consider a single weighted time constant rather than these two time constants. This new time constant is used to compare the results for different tests. This single time constant is defined such that the time it takes a transient variable to approach 63.2% of the difference between initial and final values as defined in equation (2.23):

$$\Phi_{\tau} = \Phi_{i} - 0.632\left|\Phi_{i} - \Phi_{f}\right| \tag{2.23}$$

According to this definition, the single time constant (τ) is calculated for the normalized air outlet temperature and humidity ratio. Correlations which are fitted to the normalized values and these are presented in Table 2.5 to find the single time constant. Figure 2.6 shows the single time constant values for three different Cr*. In this figure, for every Cr*, the single time constants increase as NTU increases. For most of tests, the temperature single time constant is higher than the humidity ratio time constant which shows that the system's latent transfer reaches to steady-state condition faster than the sensible energy. As it is shown in Figure 2.6, the single time constant of the LAMEE is less than an hour for all mass flow rates; however, it takes couple of hours for a RAMEE system to reach close to quasi steady-state conditions (Erb, 2009b). The slower response of the RAMEE is mainly due to two reservoirs and piping in the system (Figure 2.2) while in this paper only the LAMEE is studied and its transient response is not affected by the reservoirs nor piping.

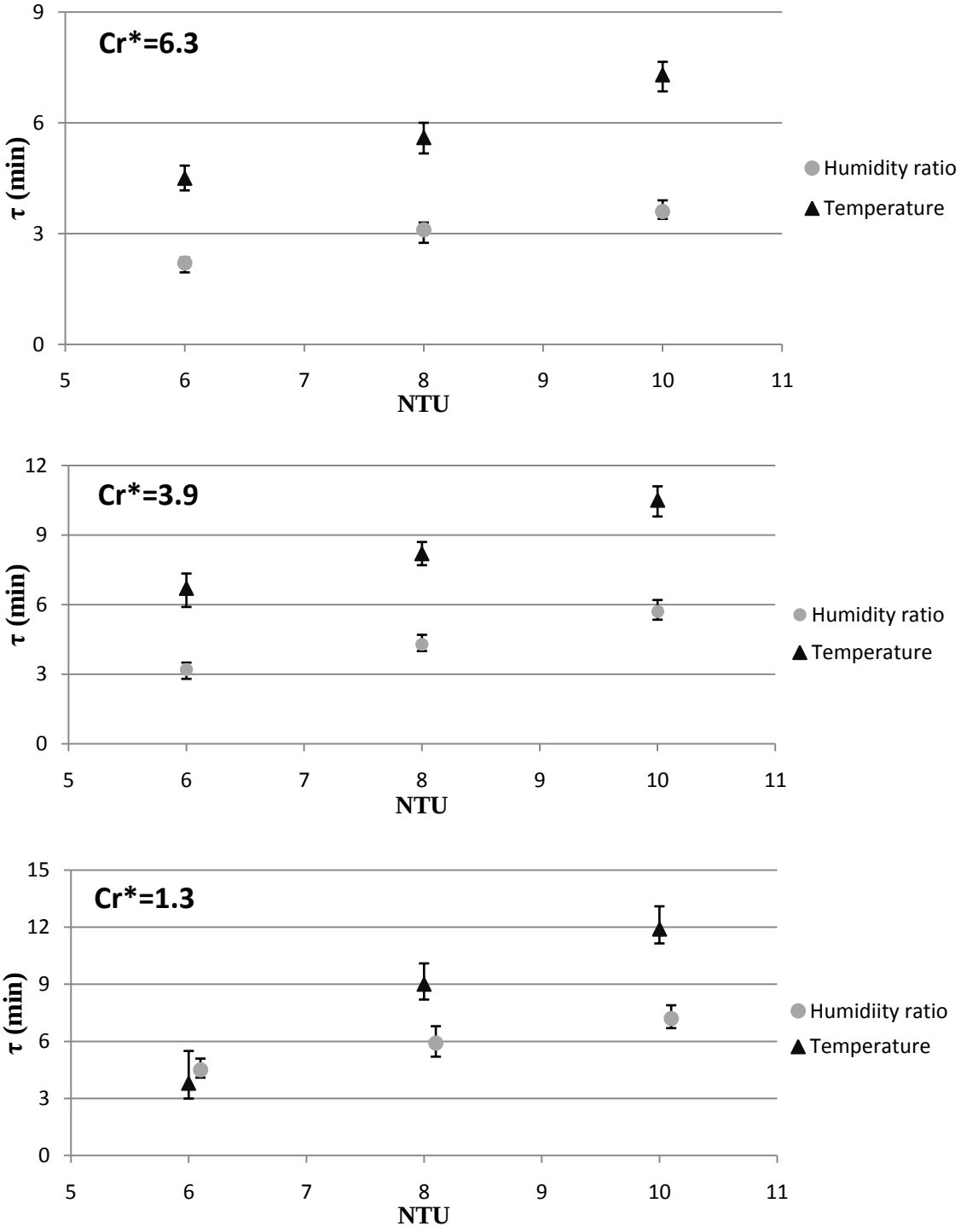

Figure 2.6 Experimental single time constants according to air outlet conditions for Cr*=6.3, Cr*=3.9, and Cr*=1.3.

The LAMEE's transient effectiveness is assessed as well. As it was mentioned in section 2.4.4, the effectiveness is the most important parameter to evaluate the performance of the LAMEE. Figure 2.7 shows the transient sensible, latent and total effectiveness for NTU=8 and Cr*=6.3 under summer standard test conditions. As it is shown all three effectiveness values increase with time and finally they reach to the steady-state values. In Figure 2.7a, the experimental data have negative values for the first three minutes which is again because of the initial conditions. Before starting the test, the liquid desiccant inside the exchanger reaches a steady-state thermal equilibrium with the airstream as it passes through the exchanger, while the air is dehumidified by the liquid desiccant. Dehumidification releases the latent heat of phase change and part of this heat is added to the airstream and, as a result, air temperature increases through exchanger and according to equation (2.2), its numerator becomes negative. Then, the liquid desiccant pump is turned on and cold desiccant enters the exchanger and the airstream cools down through the exchanger and sensible effectiveness's sign starts out negative and changes to positive.

According to Figure 2.7, the total effectiveness values and trends are more similar to the latent one compared to the sensible one under this particular test condition. However, the total effectiveness at steady-state for the LAMEE under summer AHRI test condition is more than 80%. Also, the uncertainty in the experimental data decreases as the test continues and approaches the minimum value of 4% at the steady-state condition.

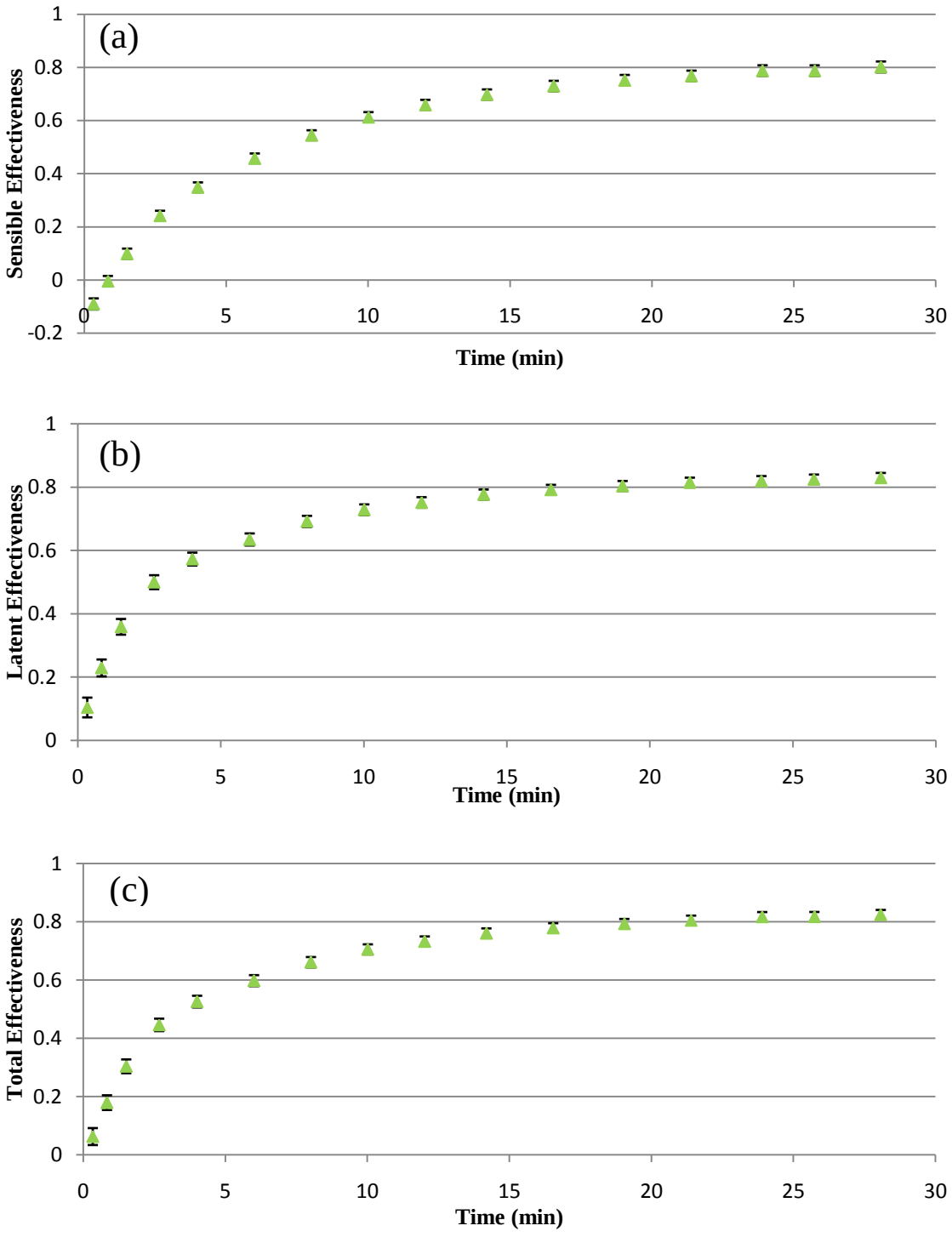

Figure 2.7 Transient (a) sensible, (b) latent, (c)total effectiveness versus time for NTU=8 and Cr*=6.3 under summer test conditions ($T_{air,\,in}$= 34˚C, $W_{air,\,in}$=25.6 g/kg).

The transient performance of the LAMEE and its effectiveness heavily depends on the initial conditions of air and desiccant inside the exchanger. Table 2.6 shows the inlet and outlet air conditions at the beginning of the test for different air and desiccant mass flow rates. The initial conditions of the air inside the exchanger are assumed to be midway between inlet and outlet conditions. As there is no desiccant flow before starting the test and the exchanger is filled by a certain mass of desiccant, it is assumed the desiccant and air inside the LAMEE are in equilibrium at the test.

Table 2.6 Air initial conditions inside the LAMEE under summer test conditions.

NTU	Cr*	$T_{air\ in}$ (˚C)	$T_{air\ out}$ (˚C)	$W_{air\ in}$ (g/kg)	$W_{air\ out}$ (g/kg)
6	1.3	35.4	35.5	24.6	25.3
	3.9	35.3	36.2	24.0	23.3
	6.3	35.3	36.6	24.5	25.2
8	1.3	34.6	38.0	27.0	27.5
	3.9	35.1	38.3	27.6	28.2
	6.3	34.0	35.5	25.6	25.8
10	1.3	35.1	36.7	26.8	26.9
	3.9	35.0	38.8	26.8	28.4
	6.3	34.7	38.1	26.4	28.2

Furthermore, the transient performance of the LAMEE is studied under winter conditions as well for a particular air and desiccant mass flow rate while the solution inlet condition is T_{sol} = 26˚C and W_{sol} = 13.3 g/kg. Figure 2.8 shows the results for NTU=8 and Cr*=3. As in the summer test conditions, the effectiveness increase with time until it reaches a steady-state value. Although the heat transfer between the LAMEE and the laboratory air is higher under winter test conditions than summer test conditions, due to higher temperature difference between the LAMEE and the lab air under winter test conditions compared to summer test conditions, the heat transfer does

not affect the sensible or latent effectiveness so much as the exchanger is insulated with a 40 mm layer of spray foam. The heat transfer between the exchanger and laboratory air affects the effectiveness less than 1% under both summer and winter test conditions.

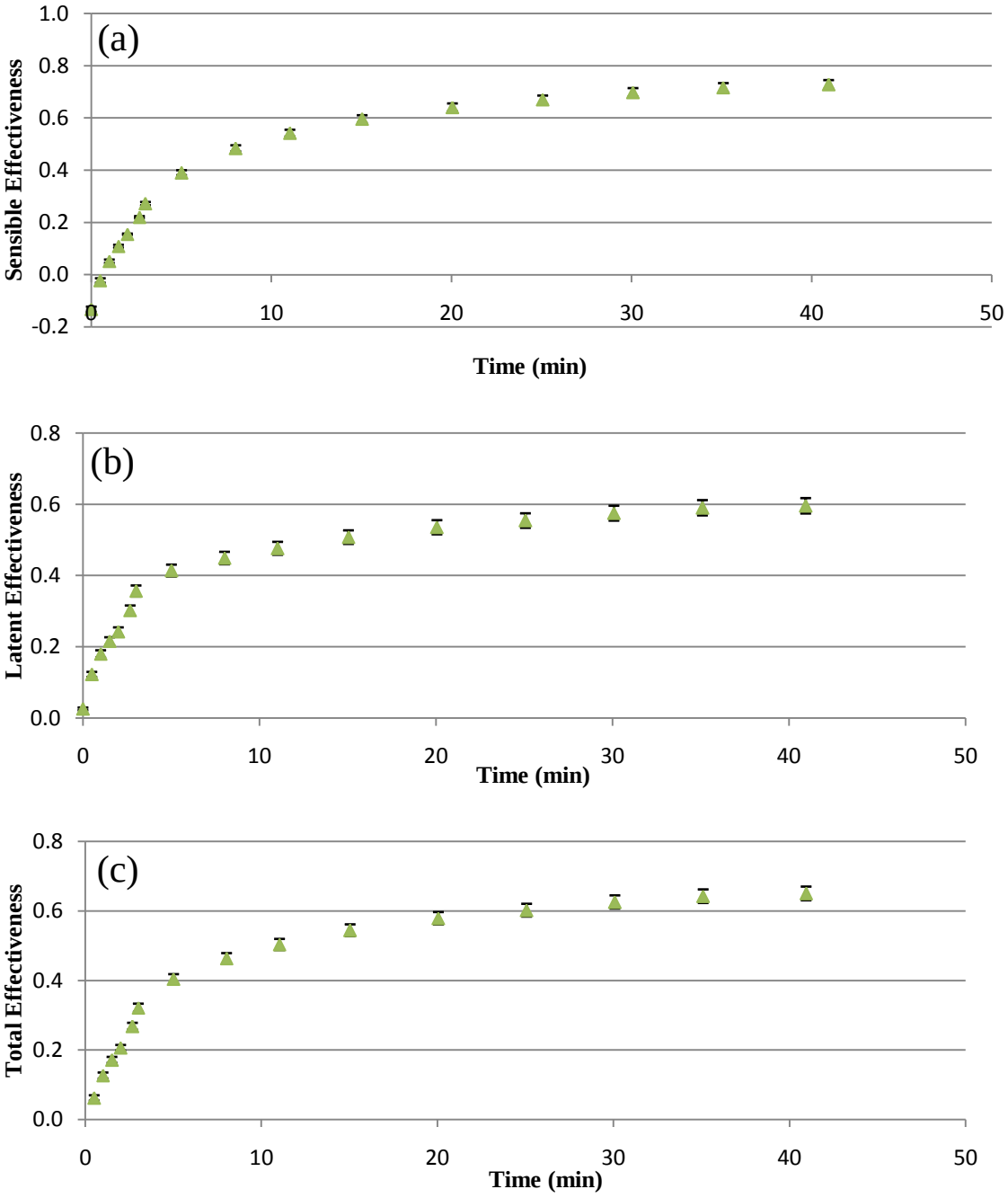

Figure 2.8 Transient (a) sensible, (b) latent, (c) total effectiveness versus time for NTU=8 and Cr*=3 under winter test conditions ($T_{air,\,in}$= 7.8˚C, $W_{air,\,in}$=3.1 g/kg).

In Figure 2.8 the effectiveness increases as the test runs and finally the total effectiveness reaches up to 65%. In Figure 2.8a these negative values at the beginning of the test again are due to initial conditions. Under winter test conditions, the buoyancy forces could have considerable impact on the LAMEE performance. In fact, under winter operating condition, when the hot desiccant flows from exchanger bottom and cooled by membrane as it flows up, the buoyancy forces could affect the LAMEE performance and this phenomenon should be assessed in detail in future research.

2.6.2 Steady-State

The steady-state performance is usually considered more important by manufacturers as the system operates many more hours close to this condition. Several parameters play role in the steady-state performance, but NTU and Cr* are the most important ones. Alternatively, the mass flow rate ratio (m*) may be used (especially for latent effectiveness) but Cr* is chosen in this paper. As it was mentioned in section 2.4.4, the relationship between Cr* and m* is nearly constant for the tests presented in this paper. Sensible, latent and total effectiveness of the LAMEE are calculated and plotted for various air and liquid mass flow rates. Figure 2.9 shows the experimental data (for nine experiments) for various NTU and Cr*. The air and desiccant inlet condition is kept almost the same for all these experiments. The average solution inlet condition is T_{sol} = 25˚C and W_{sol} = 11.6 g/kg and the average air inlet condition is close to the summer standard test conditions.

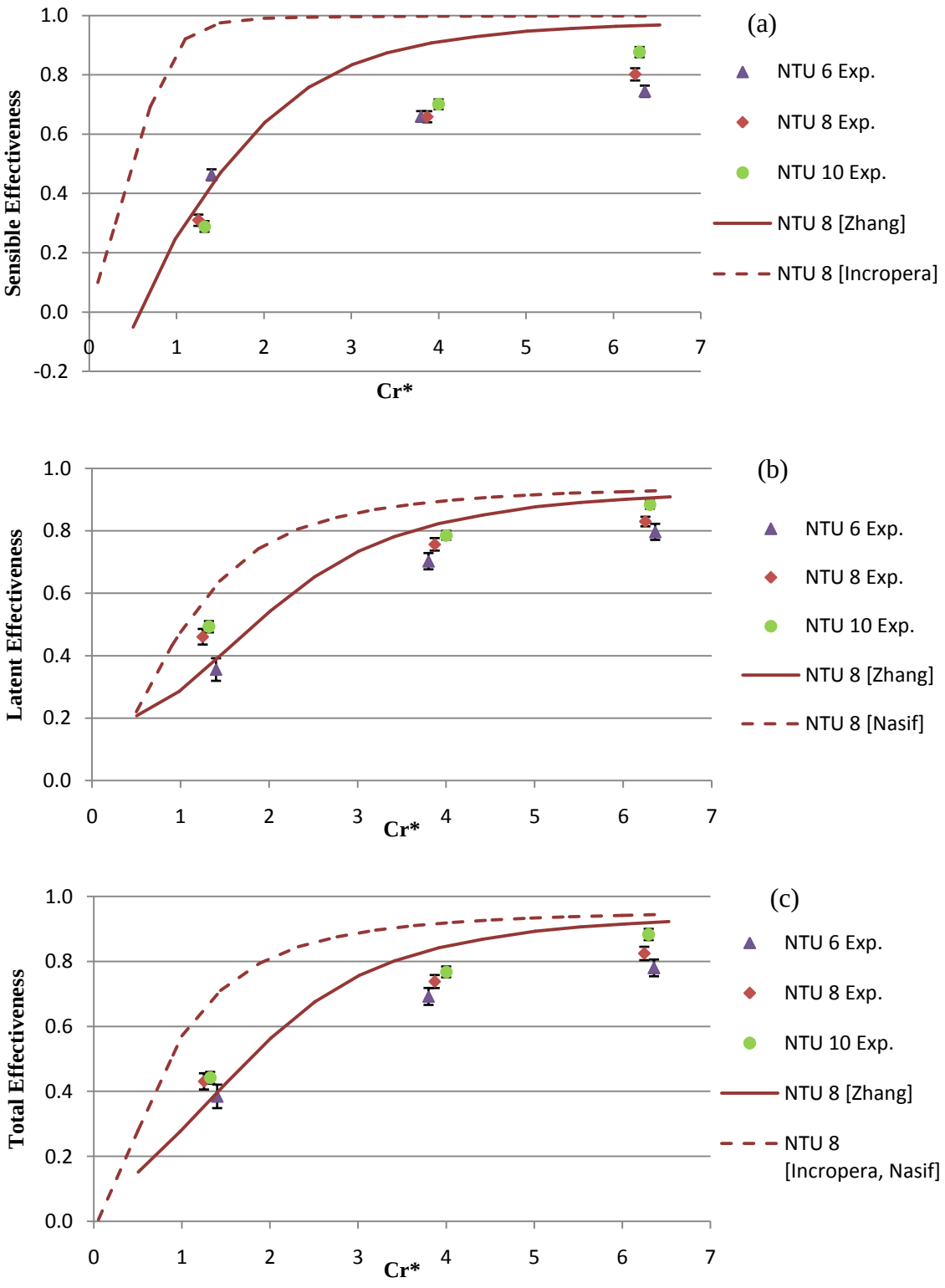

Figure 2.9 Steady-state (a) sensible, (b) latent, (c) total effectiveness versus Cr* for summer standard test condition.

In Figure 2.9, experimental data are compared to two analytical solutions. Incropera and Dewitt (2002) effectiveness correlations for a single counter flow heat exchanger are used to calculate the sensible effectiveness. According to Figure 2.9, the analytical solution for heat exchangers (Incropera and Dewitt, 2002) predicts higher sensible effectiveness values compared to experimental ones for the entire range of Cr*; however, the latent effectiveness (Nasif et al., 2005) shows better agreement. Also, the total effectiveness is calculated by equation (2.4) and using analytical definitions of sensible and latent effectiveness. The higher analytical values are due to several assumptions in the analytical solution that are different from the experiments. These include: (a) the correlations are for a counter flow configuration while the experimental LAMEE is a counter-cross exchanger, (b) the correlations are for heat transfer alone, while the LAMEE has coupled heat and moisture transfer and (c) the correlations are for uniform flow in the exchanger, while the LAMEE will have some non uniform flow due to variation channel spacing and membrane bulging (Hemingson et al., 2011b). The analytical results are developed only for NTU = 8 and NTU_m = 3.4 as the analytical solution is not sensitive to NTU and NTU_m variations in this range.

Figure 2.9 also includes results using the analytical solution of Zhang (2011) for the LAMEE tested in this paper with the VDR value of the membrane and the specific operating conditions. The Zhang solution is modified for a flat plate exchanger and the LAMEE's characteristics, VDR value of the membrane and operating conditions are given as inputs to the Zhang (2011) analytical solution and the results are presented in Figure 2.9. The predicted effectiveness of Zhang's solution is higher than the experimental data for Cr*=3.9 and Cr*=6.3, but it is closer to the experimental values

for tests with Cr*=1.3. The difference between experimental data and Zhang's analytical solution is up to 20%. These results are for NTU = 8, but this solution is not very sensitive to NTU variation over the range of NTU studied in the experiment. If NTU changes from 6 to 10 in the Zhang model, the effectiveness changes less than 5% on average.

As it is shown in Figure 2.9, both experimental and analytical data reveal that the effectiveness (sensible, latent and total) increases as Cr* increases. Also, the effectiveness increases generally as NTU increases. The only cases where the steady-state effectiveness does not correlate with NTU is the sensible effectiveness for Cr*=1.3. It is possible that the LAMEE had not reached steady-state for these tests with low liquid desiccant flow rates. Indeed longer test times are required for tests with Cr*=1.3 and there is a higher uncertainty for these tests. In addition, Figure 2.9 shows that the LAMEE is more sensitive to Cr* at lower Cr* values. For example in Figure 2.9a, with NTU=8 the sensible effectiveness increases by about 40% when Cr* increases from 1 to 3, but the sensible effectiveness increases less than 15% when Cr* increases from 3 to 5.

2.7 Conclusions

In this research, the transient characteristics of the LAMEE are investigated experimentally and its steady-state performance is assessed as well. The LAMEE consists of semi-permeable membranes and both heat and moisture can be transferred between air stream and liquid desiccant. The membrane of the LAMEE in this study is AY Tech. ePTFE and the liquid desiccant is $MgCl_2$.

The LAMEE time constant is assessed under summer test conditions for various NTU and Cr* values. For describing transient air outlet conditions, an exponential

correlation with two time constants is fitted to the measured data. The first time constant is 1-4 min and it is related to the desiccant transport time in the LAMEE while the second time constant is 5-24 min which is related to the thermal mass capacity of the LAMEE. The time constant values increases as Cr* decreases or NTU increases. The LAMEE responds faster for higher air and desiccant mass flow rates.

Also, the transient performance of the system under summer and winter operating condition is assessed and the results indicate that both latent and sensible effectiveness increase during the transient period and finally they reach a steady-state value. Under winter operating conditions, as the hot liquid desiccant is passed from the bottom to the top of the exchanger, it is cooled by the membrane and the top liquid is cooler than bottom which causes buoyancy forces to alter the results. These forces could affect the LAMEE transient performance which should be investigated in future research.

Finally, steady-state data under summer operating conditions is investigated experimentally. Also, these experimental data are compared to analytical solutions and there is 10-20% difference between Zhang's analytical solution and experimental data, but the trends are similar. The maximum experimental total effectiveness for the LAMEE under summer operating condition is 88% for NTU=10 and Cr*=6.3. Both experimental and analytical data reveal that steady-state effectiveness values increase as either Cr* or NTU increase. In conclusion, the higher Cr* values result in higher effectiveness and faster response of the system while higher NTU values lead to higher effectiveness but slower response time. In fact, higher effectiveness does not mean slower response and the response time depends on the Cr* and NTU.

CHAPTER 3

NUMERICAL MODEL VERIFICATION AND EXTRAPOLATION

3.1 Overview of Chapter 3

This chapter contains manuscript # 2 that studies the LAMEE performance experimentally and numerically. The main objective of this chapter is to verify a numerical model using experimental data from chapter 2 to predict the LAMEE transient and steady-state characteristics. The numerical model uses the finite difference method with an implicit time step to solve the heat and moisture transfer governing equations. The LAMEE thermal mass capacity and heat loss from sides are considered in the model.

To verify the numerical code, transient sensible, latent and total effectiveness data are presented versus time for different air and liquid desiccant mass flow rates and numerical data are compared with experimental data. Both the transient effectiveness and the experimental and numerical time constants are compared. Finally, the effect of air and desiccant mass flow rates on the LAMEE steady-state performance is assessed experimentally and numerically. The verified numerical model is used to investigate the impact of initial conditions on the LAMEE transient response and to determine the uncertainty in experimental data due to uncertainties in the initial conditions. Moreover, the effect of outdoor air conditions on the LAMEE time constants and steady-state effectiveness are studied numerically.

Manuscript #2: Transient heat and moisture transfer characteristics of a liquid-to-air membrane energy exchanger (LAMEE) model verification and extrapolation

Ramin Namvar, Carey J. Simonson*, Robert W. Besant

3.2 Abstract

In this paper, a transient numerical model for a liquid-to-air membrane energy exchanger (LAMEE) is developed and the results are compared to the experimental data. The data for the sensible, latent and total effectiveness are compared with transient and steady-state simulations for various values of NTU and operating parameters (Cr*, inlet temperature and humidity) while the exchanger undergoes a step change in inlet conditions and reaches a new steady-state. The transient and steady-state performances are shown to be a function of the design and operating parameters. The paper also shows that buoyancy forces become important and affect the LAMEE performance under certain operating conditions. The verified numerical model is used to investigate the impact of outdoor air conditions on the LAMEE performance.

3.3 Introduction

The steady-state response of energy exchangers has been widely studied in literature. Energy exchangers operate in steady-state conditions when the inlet and outlet conditions of two fluids are constant over time. For steady-state conditions, an analytical solution for the heat and mass transfer in a liquid-to-air membrane energy exchanger (LAMEE) was developed by Zhang (2011). The equations were described for the heat and mass transfer through the membrane from the air to the liquid desiccant. In addition to analytical solutions, the steady-state performance of the LAMEE was analyzed experimentally and numerically in (Chiari, 2000; Bergero and Chiari, 2001) and the effects of different air and desiccant mass flow rates on the steady-state performance

were investigated. Moreover, the impact of various supply air inlet conditions on a steady-state performance of a run-around membrane energy exchanger (RAMEE) was studied by Hemingson et al. (2011a). However, the transient response of the LAMEE is important for the control of LAMEEs especially when LAMEEs are combined with other equipment in an HVAC system (Rasouli et al., 2010c) as transient effects may mean that HVAC system is unable to maintain indoor comfort conditions during system start-up each morning (Namvar et al., 2012; Djongyang et al., 2010).

Although more research quantifying the transient response of the energy exchangers that transfer both heat and moisture is required because there are few publications in the literature, there are many published studies on the transient response of the heat exchangers that transfer sensible energy only. Most of these studies describe the transient response of heat exchangers after a step change in fluid mass flow rates or inlet temperatures. The system governing equations are solved numerically or analytically (e.g., using Laplace transforms) (Yin and Jensen, 2003). A survey of available heat exchanger transient response solutions and the range of parameters for which each solution is valid is presented in Bunce and Kandlikar (1995).

Recently, the transient performance of a run-around membrane energy exchanger (RAMEE) has been assessed numerically and experimentally. This system is comprised of two liquid-to-air membrane energy exchangers (LAMEE), two storage tanks and connecting tubing. The transient response of the RAMEE was assessed experimentally for different air and desiccant mass flow rates under summer and winter test conditions (Erb et al., 2009a). Seyed-Ahmadi (2009a) developed a numerical model for coupled heat and moisture transfer in the RAMEE to simulate the transient response of this

system. The two-dimensional model was developed using an implicit formulation. The transient response of the RAMEE was assessed for different air and desiccant mass flow rates and for step changes in air inlet conditions. Seyed-Ahmadi compared the numerical results to the published experimental data in (Erb et al., 2009a) and there was an acceptable agreement between numerical and experimental data. According to these results the transient response of the RAMEE heavily depends on the storage volume ratio and the initial salt solution concentration (Seyed-Ahmadi et al., 2009b).

In thermal systems, time constants are important parameters that quantify the transient response of the system (including heat and energy exchangers). The dynamic behavior of a double-pipe heat exchanger exposed to a sudden step change in flow rate was approximated by a first order response with a single time constant for each fluid stream by Abdelghani-Idrissi et al. (2001). The hot fluid which is subjected to the flow rate step change presents a decreasing time constant in flow direction; however, the cold fluid which is not subjected to the flow rate step change showed two different types of transient response. The cold fluid transient response presented an increasing time constant along the longitudinal axis of the heat exchanger or it showed uniform time constant along the axis of the heat exchanger. Lachi et al. (1997) investigated the transient behavior of a shell and tube heat exchanger using a two parameter model with a time lag and time constant. The time constant was obtained analytically, but the time lag must be determined experimentally. It was assumed that the time constant has the same value for both fluids and an analytical expression was developed for the time constant using energy balance equations. This analytical expression showed that the time constant depends on the initial and final exit bulk temperatures which are a function of the initial

and final entrance bulk temperatures and steady-state flow rates. Generally, the results revealed that the time constant decreases as the flow rate or flow rate step increases. The range of time constant for heat exchangers is less than a minute in these studies (Abdelghani-Idrissi et al., 2001; Lachi et al., 1997), however, LAMEEs show longer time constants due to their large thermal and moisture capacities and the coupled heat and moisture transfer that occurs in LAMEEs (Namvar et al., 2012).

The buoyancy forces impact on heat exchanger performance is an important topic and has been studied in many researches. The LAMEE performance might be affected by buoyancy forces due to temperature difference between the membrane surface and liquid desiccant. In winter operating conditions, the hot liquid desiccant entered from exchanger bottom and was cooled by the membrane and the air flow as it flows up. The density difference between top cooled liquid and bottom hot liquid could affect the flow distribution in the liquid channel with a reduction in the LAMEE performance. The natural convection between parallel plate flows has been studied for various applications in the cooling of electronic equipment, heat exchangers and nuclear reactors. Elenbaas (1942) first conducted an experiment on the natural convection between two parallel vertical plates and his work was followed by many numerical and experimental works for both laminar and turbulent flow regimes. A review of available models and correlations for natural convection heat transfer between vertical parallel plate channels is presented in (Teertstra, 1997).

The main purpose of this research is to investigate transient response of a LAMEE under summer and winter operating conditions. The numerical results are compared to the published experimental data (Namvar et al., 2012) and the numerical

model is verified. The verified numerical model is used to investigate the transient response and steady-state performance of the LAMEE for different operating conditions.

3.4 The LAMEE

Figure 3.1 shows a counter-cross LAMEE tested (1.218m length, 0.305m height and 0.1m width). The LAMEE is constructed with ten rectangular panels; each panel consists of two semi-permeable Ay-tech ePTFE membranes to contain the liquid which allow water vapor to pass through, but not liquid water. Thus, both heat and water vapor are able to be transferred between the air and liquid flows. The LAMEE and its membrane properties are presented in Table 3.1.

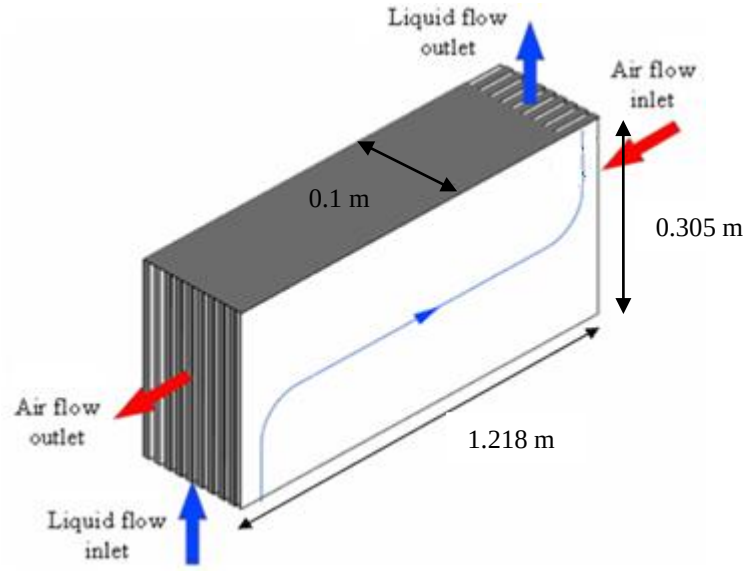

Figure 3.1 The counter-cross flow liquid-to-air membrane energy exchanger (LAMEE) studied in this paper showing the dimensions and one liquid streamline (Namvar et al., 2012; Beriault , 2010).

Table 3.1 The LAMEE dimensions and properties.

LAMEE Properties	
Exchanger length (m)	1.218
Exchanger width (m)	0.305
Number of panels	10
Aspect ratio (L/W)	4
Air gap thickness (mm)	6.35
Solution gap thickness (mm)	3.17
Solution inlet length (m)	0.066
Specific heat capacity (J/kg˚K)	1.16
Total mass (kg)	28
Membrane type	ePTFE-AY Tech
Mass resistance of membrane (s/m)	97
Membrane thermal conductivity (W/m)	0.334
Membrane thickness (mm)	0.54

In order to evaluate the LAMEE performance, the effectiveness is used as the most important parameter in energy recovery systems according to ASHRAE Standard 84 (ANSI/ASHRAE, 2008). In this paper, the LAMEE performance is evaluated by the sensible, latent and total effectiveness (ε_s, ε_l, ε_t). If effectiveness is used without a qualifier, then it refers to all three effectivenesses. The sensible effectiveness quantifies the sensible heat transfer fraction between the air flow and the liquid desiccant flow. When the thermal capacity rate of the air is lower than the thermal capacity rate of the desiccant, the sensible effectiveness is calculated from:

$$\varepsilon_{\mathrm{S}} = \frac{(T_{\mathrm{air,in}} - T_{\mathrm{air,out}})}{(T_{\mathrm{air,in}} - T_{\mathrm{sol,in}})} \tag{3.1}$$

The latent effectiveness represents the ratio of actual to maximum possible transfer moisture (or latent energy when the heat of phase change is constant) between the air and liquid desiccant flows. When the mass flow rate of the air is lower than the mass flow rate of the liquid desiccant (as it is in this paper), the latent effectiveness can be calculated from:

$$\varepsilon_{\mathrm{L}} = \frac{(W_{\mathrm{air,in}} - W_{\mathrm{air,out}})}{(W_{\mathrm{air,in}} - W_{\mathrm{sol,in}})} \tag{3.2}$$

The total effectiveness depends on both heat and moisture transfer and it is calculated from following equation (Simonson and Besant, 1999):

$$\varepsilon_{\mathrm{T}} = \frac{\varepsilon_{\mathrm{S}} + H^{*}\varepsilon_{\mathrm{L}}}{(1 + H^{*})} \tag{3.3}$$

where H* is the operating factor which depends on the air and liquid desiccant inlet conditions (Simonson and Besant, 1999):

$$H^{*} = \frac{\Delta H_{L}}{\Delta H_{S}} = 2500\,\frac{W_{air,in} - W_{sol,in}}{T_{air,in} - T_{sol,in}} \tag{3.4}$$

Two important dimensionless parameters, number of heat transfer units (NTU) and ratio of heat capacity rates (Cr*) are defined for each test and these numbers characterize the air and desiccant mass flow rates for the test.

$$Cr^* = \frac{C_{sol}}{C_{air}} \tag{3.5}$$

$$NTU = \frac{UA}{C_{\min}} \tag{3.6}$$

where U is the overall heat transfer coefficient ($W/(m^2K)$), A is the membrane surface area (m^2), C_{Sol} and C_{air} are the heat capacity rates of desiccant solution and air, respectively, and C_{min} is the minimum value of C_{sol} and C_{air}.

3.5 Numerical Model

3.5.1 The Numerical Model Structure

A numerical model is developed to analyze the LAMEE steady-state and transient performance and the experimental results will be compared to these numerical data. This model has been developed based on conservation of energy and moisture in two coupled control volumes, one for the airstream and one for the liquid desiccant stream (Hemingson et al., 2011a, Seyed Ahmadi, 2008c). In this paper only a summary of the model and modifications are presented. The model is based on the finite difference method with an implicit time step according to two-dimensional heat and moisture transfer equations in the LAMEE. To simplify the governing equations some assumptions are used in the governing equations (Hemingson et al., 2011a; Erb et al., 2009a):

1. The liquid desiccant and air are considered as laminar and fully developed flows.
2. The membrane properties are constant with temperature and relative humidity (Larson et al., 2007)

3. The heat and moisture transfer occur only in the normal direction to each membrane.
4. Axial heat conduction and water vapor molecular diffusion of the fluids in the flow direction are negligible.
5. The desiccant liquid properties in the storage tank are assumed to be constant and uniform.
6. The membrane heat and mass transfer capacitance effects are negligible (Iskara, 2007).

According to these assumptions, the governing equations for the moisture and heat transfer in the LAMEE are:

$$\rho_{dAir}\delta_{Air}\frac{\partial W_{Air}}{\partial t}=-2U_m^{'}\left(W_{Air}-W_{Sol,mem}\right)-J_{dAir}\bullet\nabla W_{Air}\delta_{Air} \tag{3.7}$$

$$\rho_{Salt}\delta_{Sol}\frac{\partial X_{Sol}}{\partial t}=2U_m^{'}\left(W_{Air}-W_{Sol,mem}\right)-J_{Salt}\bullet\nabla X_{Sol}\delta_{Sol} \tag{3.8}$$

$$\rho_{Air}Cp_{Air}\delta_{Air}\frac{\partial T_{Air}}{\partial t}=2\cdot\left[-U\left(T_{Air}-T_{Sol}\right)+U_m^{'}\left(W_{Air}-W_{Sol,mem}\right)h_{fg}\left(1-\eta\right)\right]-J_{Air}\bullet\nabla T_{Air}Cp_{Air}\delta_{Air} \tag{3.9}$$

$$\rho_{Sol}Cp_{Sol}\delta_{Sol}\frac{\partial T_{Sol}}{\partial t}=2\cdot\left[U(T_{Air}-T_{Sol})+U_m^{'}\left(W_{Air}-W_{Sol,mem}\right)h_{fg}\,\eta\right]-J_{Sol}\bullet\nabla T_{Sol}Cp_{Sol}\delta_{Sol} \tag{3.10}$$

This model is able to determine the steady-state and transient responses of a LAMEE in terms of effectiveness for a given operating conditions. The model calls the air and liquid desiccant inlet conditions and properties to solve the governing equations until they converge for each test with different operating conditions. The LAMEE

dimensions and its membrane properties are defined in the code and they are assumed to be constant for all tests. Also, the heat transfer between the LAMEE and laboratory environment is considered in the model (Seyed-Ahmadi et al., 2009a), but its impact on the results is negligible as the LAMEE is insulated with a 40mm layer of spray foam. The effectiveness changes less than 1% due to heat transfer between the LAMEE and laboratory air.

3.5.2 Thermal mass capacity

Prior to start-up of a HVAC system or any process including a LAMEE, the LAMEE will be in thermal equilibrium with the surrounding ambient air. As the process begins and the air and liquid begin to flow through the exchanger, the thermal mass capacity of the exchanger can have a large impact on its transient performance as it will take time for the LAMEE structure to reach steady-state with the air and desiccant flowing through the LAMEE. The thermally dominant materials in the LAMEE studied in this paper (Figure 3.1) are aluminum and plastic and its total mass is around 28 kg and its effective specific heat capacity is C_P =1.16 J/kg·K. The LAMEE thermal mass capacity is incorporated in the air thermal capacity using a correction factor f. This correction factor converts the LAMEE thermal mass capacity to equivalent air thermal mass:

$$(1+f)\rho_{Air}Cp_{Air}\delta_{Air}\frac{\partial T_{Air}}{\partial t}=2\cdot\left[-U\left(T_{Air}-T_{Sol}\right)+U'_m\left(W_{Air}-W_{Sol,mem}\right)h_{fg}\left(1-\eta\right)\right]-J_{Air}\bullet\nabla T_{Air}Cp_{Air}\delta_{Air} \quad (3.11)$$

where:

$$f = M\exp(-t/t_{ex}) \quad (3.12)$$

$$t_{ex} = \frac{M_{ex} C_{P,ex}}{h_{air} A_{ex}} \tag{3.13}$$

The correction factor is an exponential correlation with two constants. The constant M depends on the LAMEE mass, aspect ratio and specific heat capacity and it shows the ratio of the LAMEE thermal mass capacity to the air thermal mass capacity. According to construction drawings of the LAMEE studied in this paper (Beriault, 2010), the mass distribution is not uniform among 10 channels in the LAMEE and almost half of its mass is in the two outside channels on each side of the exchanger while other half of the mass is distributed uniformly among other 8 channels. The second constant is a time delay (t_{ex}) which is calculated in equation (3.13) and it is found to be 25±3 min for the exchanger modeled in this paper. This value shows how quickly the LAMEE structure responds to the temperature change at start-up.

Figure 3.2 shows the impact of considering thermal mass capacity of the LAMEE in the numerical code for a selected case with: NTU=8, Cr*=6.3, air inlet conditions of 34°C and 25.6 g/kg and liquid desiccant inlet conditions of 24.4°C and 10.8 g/kg. The initial conditions of the air and desiccant at all points in the LAMEE are assumed to be equal to the inlet air conditions. As shown in Figure 3.2, this modification only affects the transient results and it does not have considerable impact on the steady-state results. In addition, the sensible effectiveness is more affected by the LAMEE thermal mass capacity compared to the latent one. In fact, the latent effectiveness is affected only because of coupling of heat and moisture transfer (Hemingson et al., 2011a). Considering thermal mass capacity affects the transient

sensible effectiveness up to 30% while the latent effectiveness will be changed less than 5%. Thus, the LAMEE thermal mass capacity is implemented in the governing equations and it is considered for all following numerical data.

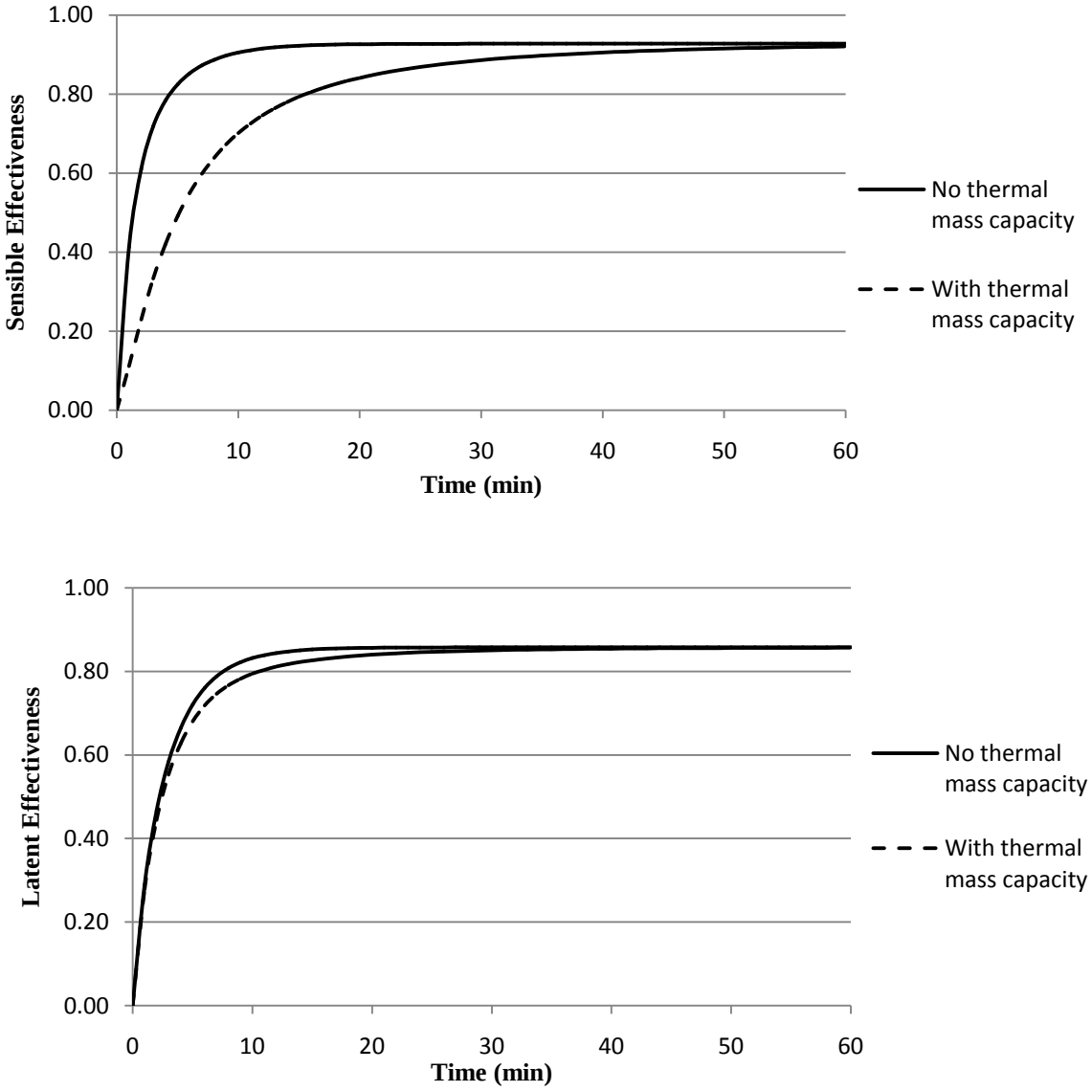

Figure 3.2 Numerical sensible and latent effectiveness of the LAMEE with and without considering the thermal mass capacity in the numerical model for NTU=8 and Cr*=6.3.

3.5.3 Time Step and Domain Discretization

The time step used in the numerical model should be small enough to get a time accurate solution for the transient response of the LAMEE. On the other hand, the lower the time step value, the longer the computer run time. Changing the time step from 5s to 60s changes the transient effectiveness values by less than 0.5%. Thus, Δt= 10s is chosen as the time step according to sensitivity study on the time step. In this code, the first order time step discretization is used, but even using a second order time step discretion does not affect the results significantly and the effectiveness values will be changed less than 0.3%. Moreover, the number of nodes on the panel should be high enough to ensure that the results are not sensitive to number of nodes in x and y directions. For the LAMEE used in this paper, it is assumed $\Delta x=\Delta y$ and according to the LAMEE length and height the number of nodes is 204×51 which is selected according to sensitivity study on the mesh size. If the number of nodes is doubled (408×102), the effectiveness values will be changed less than 0.2%. However, if the half number of nodes are used (102×25) the steady-state sensible and latent effectiveness decrease 4% and 3%, respectively.

3.5.4 Buoyancy Forces

The LAMEE performance is considered in both summer and winter test conditions. The summer test condition occurs when the air is cooled and dehumidified (i.e. the desiccant is heated and humidified) in the LAMEE, while the winter test condition occurs when the air is heated and humidified (i.e. the desiccant is cooled and dehumidified). In the experiments, the desiccant flow through the LAMEE is from the bottom to the top as it is shown in Figure 3.3.

As the desiccant flows from the bottom to the top, it is heated and humidified during the summer and cooled and dehumidified during the winter. Therefore during the winter test conditions, the desiccant is cooled by the membrane as it flows up and this cooled liquid desiccant will be denser than hot bottom liquid desiccant and buoyancy forces might play important role under this condition.

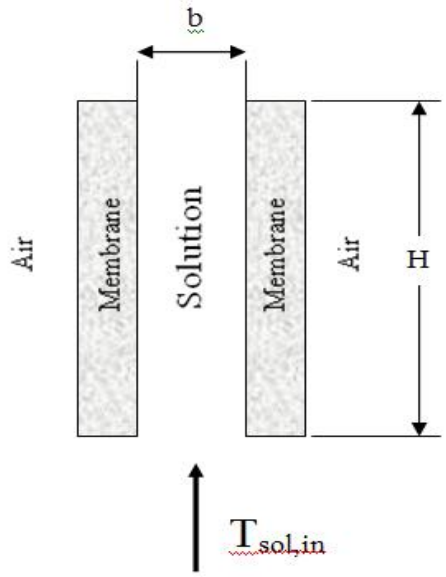

Figure 3.3 Schematic of a desiccant solution channel in the LAMEE.

In addition, the natural convection will be larger under winter test conditions when the temperature differences are larger. To investigate this phenomenon some classical non-dimensional parameters such as Grashof and Richardson numbers are investigated numerically. The Grashof number is a ratio of buoyancy to viscous forces. If a desiccant channel of the LAMEE is assumed to be a vertical isothermal channel, the Grashof number is defined as:

$$Gr = \frac{g\beta(T_{mem} - T_{in,sol})b^3}{\upsilon^2} \tag{3.14}$$

Also, the Richardson and Reynolds numbers are defined in equations (3.15)and (3.16):

$$Ri = \frac{Gr}{\mathrm{Re}^2} \tag{3.15}$$

$$\mathrm{Re} = \frac{U_0 b}{\upsilon} \tag{3.16}$$

Richardson number is an important number to investigate the combined forced and free convection. When Richardson number is less than 1.0, forced convection plays more significant role in heat transfer, but natural convection is dominant mode of heat transfer when the Richardson number is more than 10 (Teertstra, 1997).

3.6 Experiments

3.6.1 Experimental Data

The published experimental data (Namvar et al., 2012) are used to verify the numerical model. The LAMEE is the main part of the experimental set-up and the experiment provides constant air and desiccant conditions at the inlet of the LAMEE from t=0 to the time when steady-state occurs. The facility sensors measure the inlet and outlet conditions (T, RH, concentration and mass flow rate) of the air and liquid desiccant during the test. More details on experimental and test facility are available in (Namvar et al., 2012).

Before starting the test, the LAMEE is full of liquid desiccant ($MgCl_2$) and the air stream passes through the LAMEE until the air reaches to the desired inlet

conditions. Then, the liquid desiccant is pumped to the LAMEE and test starts. The mass and energy balance analysis are done for the experimental set-up. The analysis shows that the mass and energy imbalances are less than 8% and 5%, respectively (Namvar et al., 2012).

The published experimental data (Namvar et al., 2012) include the tests under both summer and winter test conditions. For summer test conditions, the air inlet temperature is between 34˚C and 35.4˚C, while its humidity ratio varies from 24.2 g/kg to 27.6 g/kg for different tests. The liquid desiccant reservoir is in the laboratory and it is in equilibrium with ambient air temperature. The air and desiccant inlet conditions for all tests with different mass flow rates under the summer test condition are shown in Table 3.2. In addition, a single test is presented under winter test conditions where the air is heated and humidified. The air inlet conditions are T=7.8˚C and W= 3.1g/kg and desiccant inlet conditions are T=26˚C and W= 13.3g/kg.

Table 3.2 The air and liquid desiccant inlet conditions under summer test conditions.

NTU	Cr*	$T_{air\ in}$ (˚C)	$W_{air\ in}$ (g/kg)	$T_{sol\ in}$ (˚C)	$W_{sol\ in}$ (g/kg)
6	1.3	35.4	24.5	25.9	13.7
	3.9	35.3	24.2	25.0	11.6
	6.3	35.3	24.3	25.1	11.7
8	1.3	34.6	26.7	25.1	11.6
	3.9	35.1	27.6	25.2	11.3
	6.3	34.0	25.6	24.4	10.8
10	1.3	35.1	26.8	23.5	10.0
	3.9	35.0	26.6	23.4	10.2
	6.3	34.7	26.3	23.4	10.1

3.6.2 Initial Conditions

The transient response of the LAMEE depends mostly on the air and desiccant initial conditions inside the LAMEE. Initial conditions show the air and desiccant temperature and humidity inside the LAMEE at t=0 and they are different from inlet conditions. The initial conditions in the published experimental data (Namvar et al., 2012) is assumed to be between the air inlet and outlet conditions at t=0. In these experiments, the air passes through the LAMEE which is filled by liquid desiccant until air reaches to the desired conditions, thus the inlet and outlet conditions of the air at t=0 are different. The liquid desiccant inside the LAMEE is in equilibrium with the flowing air as there is no desiccant flow before starting the test. Here, a sensitivity study is presented to determine the impact of initial conditions on transient response of the LAMEE.

Figure 3.4 shows the impact of the different initial conditions on the transient response of the LAMEE. In this figure the numerical transient sensible and latent effectiveness are shown for tests with same operating conditions and different initial conditions. These results show the effectiveness for NTU=8 and Cr*=6.3 and air and desiccant inlet conditions are presented in Table 3.2. Two different cases are considered as initial conditions in the code. In first case, the initial conditions are assumed to be same as air inlet conditions at t=0, T_{air}=34˚C, W_{air}=25.6 g/kg. In second case, the initial conditions are equal to air outlet conditions at t=0, T_{air}=35.5˚C, W_{air}=25.8 g/kg (Table 3.3). For both of these cases, desiccant initial conditions are equal to the air initial conditions. These results emphasize the impact of the assumed initial conditions in (Namvar et al., 2012) and they show the uncertainty in the experimental sensible and latent effectiveness values due to the uncertain initial conditions. The uncertainty is ±6%

for sensible effectiveness at time =0 and this reduces to 1% at t=25 min. The impact on the latent effectiveness is minimal in this case, but this impact could be different from test to test and it depends on the length of preconditioning time of the inlet air before starting the test.

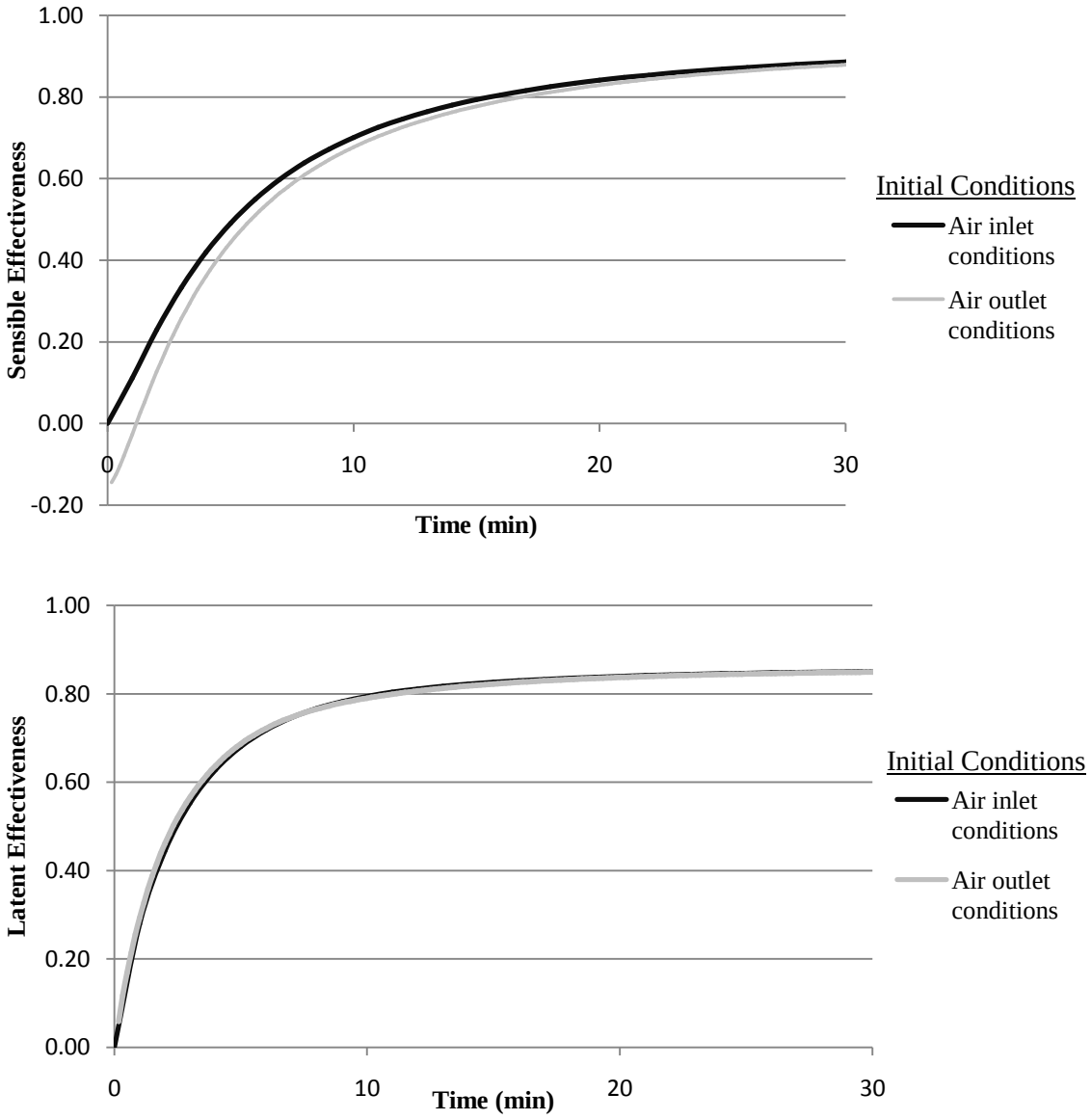

Figure 3.4 Numerical sensible and latent effectiveness for the same operating conditions (NTU=8, Cr*=6.3) but different assumptions for the initial conditions.

Table 3.3 The inlet conditions of the air entering and leaving the LAMEE under summer test conditions at t=0. The initial conditions of the air are assumed to vary linearly between the inlet and outlet conditions unless otherwise specified. The liquid desiccant is assumed to be in thermal and moisture equilibrium with the air at t=0.

NTU	Cr*	$T_{air\ in}$ (˚C)	$T_{air\ out}$ (˚C)	$W_{air\ in}$ (g/kg)	$W_{air\ out}$ (g/kg)
6	1.3	35.4	35.5	24.6	25.3
	3.9	35.3	36.2	24.0	23.3
	6.3	35.3	36.6	24.5	25.2
8	1.3	34.6	38.0	27.0	27.5
	3.9	35.1	38.3	27.6	28.2
	6.3	34.0	35.5	25.6	25.8
10	1.3	35.1	36.7	26.8	26.9
	3.9	35.0	38.8	26.8	28.4
	6.3	34.7	38.1	26.4	28.2

The air inlet and outlet conditions at t=0 are presented for all tests presented in Table 3.3. As a result, the initial conditions in the model have been assumed as a linear gradient between air inlet and outlet conditions at t=0 and this assumption has been used for all following numerical simulations in this research paper.

The sensible effectiveness shows negative values for first few minutes when the initial conditions are assumed to be same as outlet conditions. The main reason for these negative values are the air and liquid desiccant initial conditions inside the LAMEE. Before starting the test, during the preconditioning period, the air passes through the LAMEE until the air inlet conditions reaches to the steady-state and desired conditions. Meanwhile, the air is dehumidified by the liquid desiccant inside the LAMEE and this dehumidification release energy which causes the higher temperature at air outlet compared to the air inlet for first few minutes (Namvar et al., 2012).

3.7 Results and Discussions

In this paper, the transient and steady-state performance of the LAMEE will be investigated and numerical results will be compared to the published experimental data (Namvar et al., 2012). First, the LAMEE transient sensible, latent and total effectiveness are studied under both summer and winter test conditions. Then, the LAMEE time constant, as an important transient response parameter, is investigated for different tests with different air and desiccant solution mass flow rates. Following this, the verified numerical model is used to show the impact of the air inlet conditions on the time constants of the LAMEE. Finally, the steady-state performance of the LAMEE is shown for different tests for heating and dehumidifying test conditions and the effect of outdoor air conditions on the LAMEE performance will be assessed numerically.

3.7.1 Transient

3.7.1.1 Effectiveness

The LAMEE performance is mainly assessed under summer test conditions which the outdoor air is cooled and dehumidified. The transient effectiveness of the LAMEE is shown for three different tests in Figures 3.5, 3.6 and 3.7. In these tests, NTU is 8 and Cr* values are 6.3, 3.9 and 1.3. The air and desiccant solution inlet conditions for these tests are presented in Table 3.2 and the initial conditions are assumed to be linear gradient between air inlet and outlet conditions at t=0 which are presented in Table 3.3. For all of these results, the effectiveness increases as test runs until it reaches to a steady-state value and there is an acceptable agreement between experimental and numerical data. Moreover, both numerical and experimental sensible effectiveness show negative values for first few minutes due to the initial conditions of the air and liquid

desiccant at t=0. The dashed lines on the following figures indicate the uncertainty in numerical data due to uncertainty in NTU, Cr*, estimating thermal mass capacity and initial conditions.

Figure 3.5 shows the transient sensible, latent and total effectiveness for NTU=8 and Cr*=6.3 and there is very good agreement between numerical and experimental data and the maximum difference between experimental and numerical data is less than 10%. At most data points, the numerical data are within the uncertainty bars of experimental data. For sensible effectiveness, the experimental data verify the numerical data especially at beginning of the test and finally the maximum difference between them is 8%. The agreement between numerical and experimental data is even better for the latent and total effectiveness. The average difference between the numerical and experimental data in latent and total effectiveness is less than 5%.

The transient effectiveness values for Cr*=3.9 and Cr*=1.3 are shown in Figures 3.6 and 3.7, respectively. For Cr*=3.9, there is an acceptable agreement for latent and total effectiveness, but the numerical values for sensible effectiveness are higher than the experimental values. There is up to a 15% difference between the numerical and experimental data for sensible effectiveness. For the lowest Cr* value, Cr*=1.3, there is a good agreement between numerical and experimental data, but for the latent and total effectiveness, the experimental results show higher values than the numerical data.

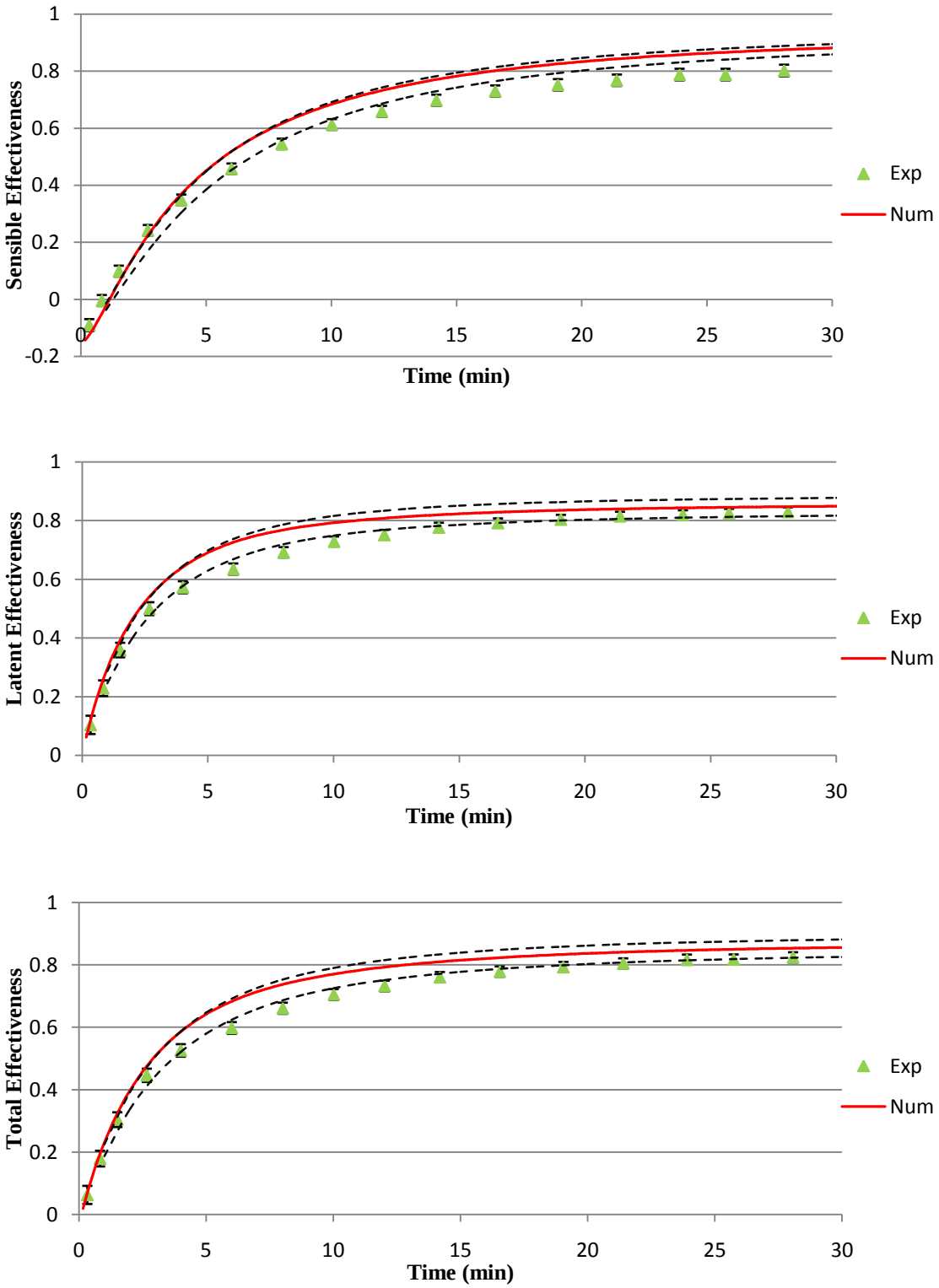

Figure 3.5 Transient sensible, latent and total effectiveness versus time for NTU=8 and Cr*=6.3 under summer test conditions ($T_{air,\,in}$= 34˚C, $W_{air,\,in}$=25.6 g/kg).

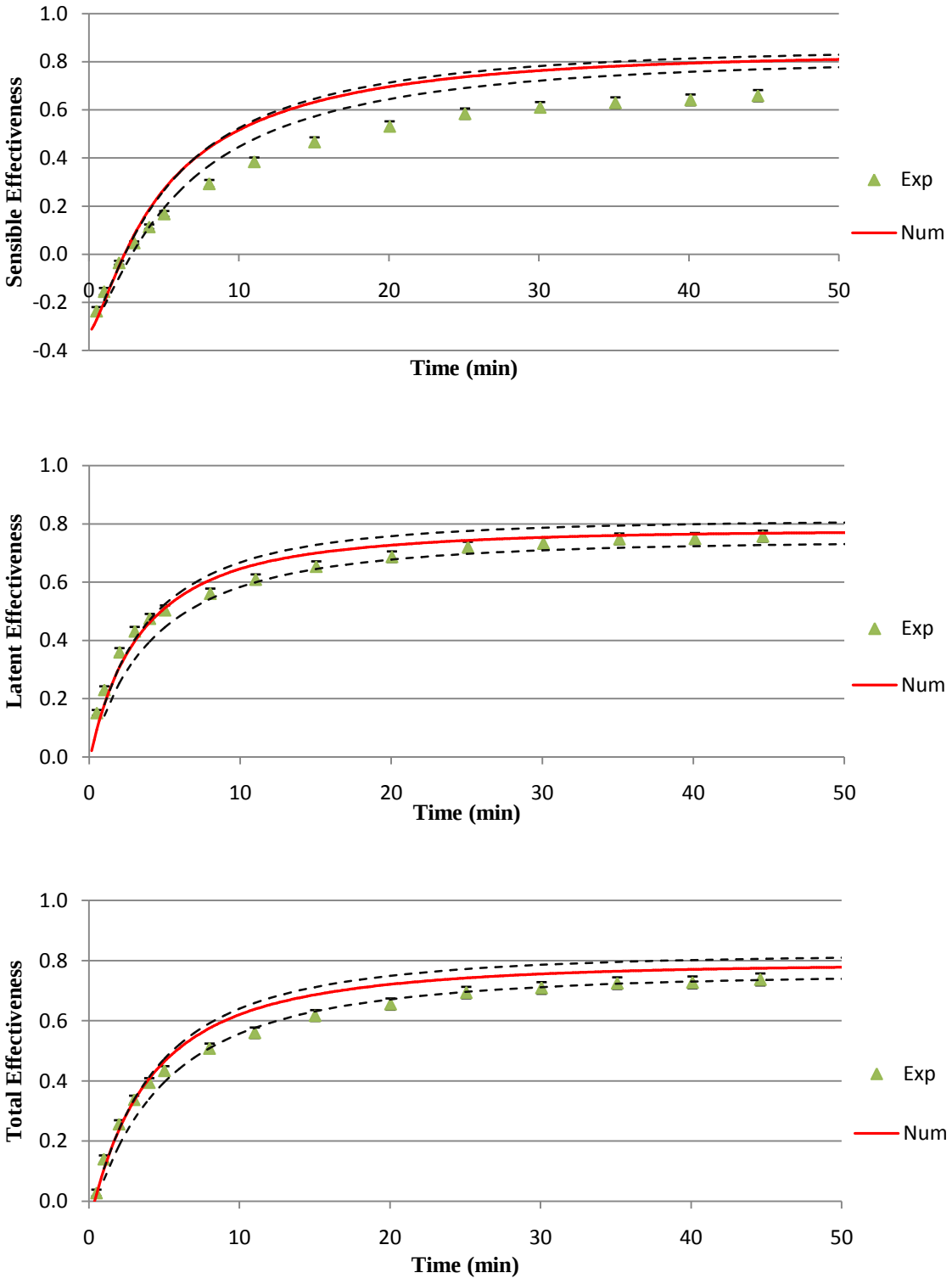

Figure 3.6 Transient sensible, latent and total effectiveness versus time for NTU=8 and Cr*=3.9 under summer test conditions ($T_{air,\,in}$= 35.1˚C, $W_{air,\,in}$=27.6 g/kg).

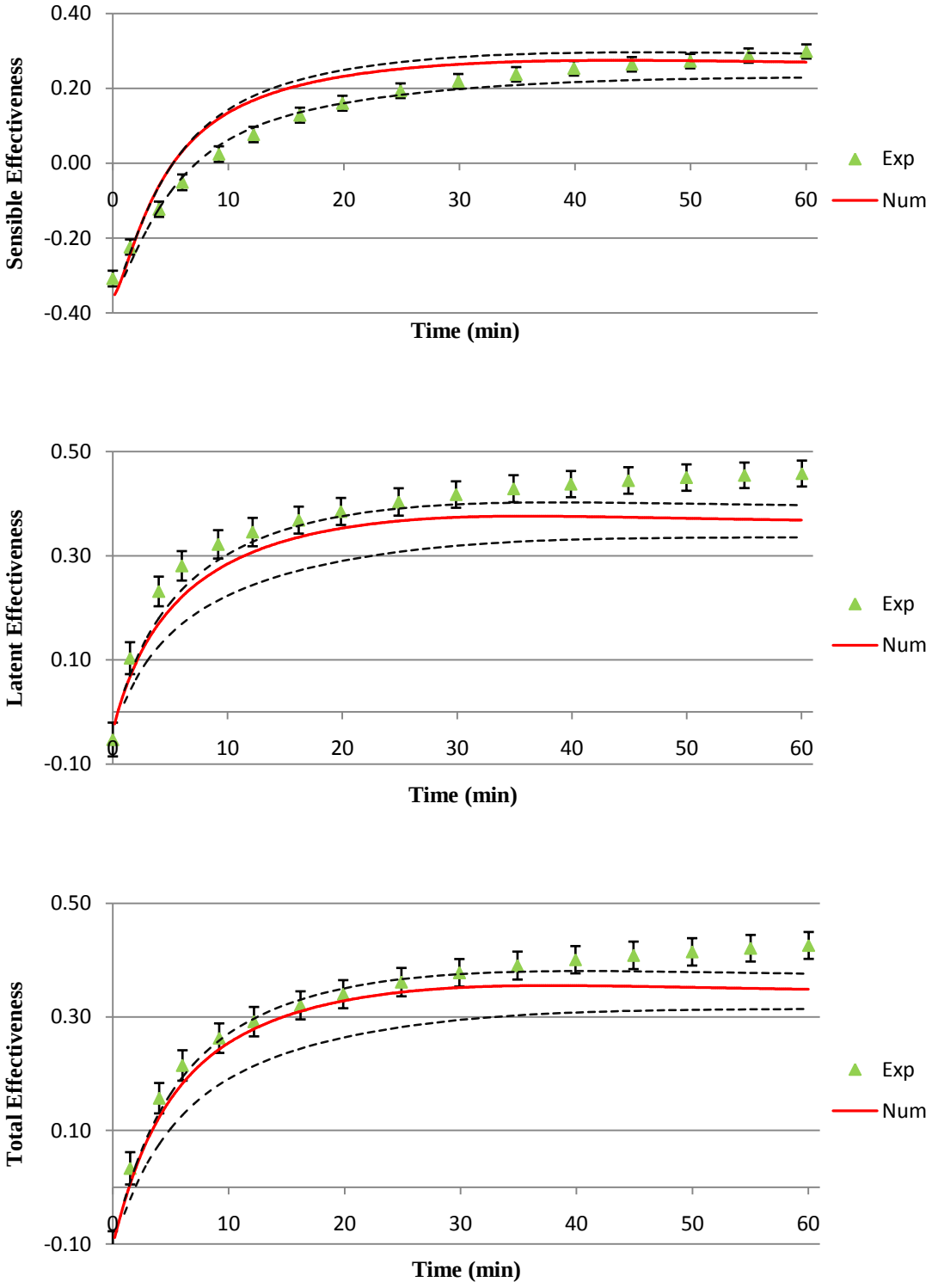

Figure 3.7 Transient sensible, latent and total effectiveness versus time for NTU=8 and Cr*=1.3 under summer test conditions ($T_{air,\,in}$= 34.6˚C, $W_{air,\,in}$=26.7 g/kg).

To quantify the difference between the experimental and numerical data, the root mean square error (RMSE) is calculated as follows:

$$RMSE = \frac{\sqrt{\sum_1^N (\varepsilon_{\text{Num}} - \varepsilon_{\text{Exp}})^2}}{N} \tag{3.17}$$

where N is the number of points in the transient data used for comparison (60 points). In addition, the average absolute difference (AAD) is used to compare experimental and numerical data and it is defined as follows:

$$AAD = \frac{\sum_1^N \left| \varepsilon_{\text{Num}} - \varepsilon_{\text{Exp}} \right|}{N} \tag{3.18}$$

The RMSE and AAD values for all the tests under summer test conditions are presented in Table 3.4. These results show that RMSE and AAD values for the sensible effectiveness are higher compared to the latent and total effectiveness which means the experimental and numerical data show better agreement for the latent and total effectiveness compared to the sensible one. In fact, the RSME and values for total effectiveness are closer to the latent effectiveness rather than sensible effectiveness since the total effectiveness trends and values are more similar to the latent effectiveness under the summer test condition. The average AAD value is less than 0.1 for the sensible effectiveness and it is less than 0.05 for the latent and total effectiveness. These values reveal that there is very good agreement between numerical and experimental data and the model is able to represent the experimental results.

Table 3.4 The root mean square error (RSME) and the average absolute difference (AAD) of effectiveness values of the LAMEE under summer test conditions.

		RMSE			AAD		
NTU	Cr*	Sen	Lat	Tot	Sen	Lat	Tot
6	1.3	0.002	0.001	0.002	0.037	0.033	0.034
	3.9	0.014	0.002	0.002	0.109	0.035	0.035
	6.3	0.005	0.000	0.000	0.068	0.015	0.012
8	1.3	0.003	0.003	0.002	0.044	0.052	0.034
	3.9	0.021	0.001	0.004	0.141	0.028	0.052
	6.3	0.004	0.002	0.003	0.063	0.044	0.047
10	1.3	0.002	0.003	0.003	0.037	0.050	0.048
	3.9	0.033	0.004	0.008	0.177	0.064	0.088
	6.3	0.021	0.006	0.009	0.140	0.077	0.090
Average		**0.012**	**0.003**	**0.003**	**0.091**	**0.044**	**0.049**

There are several reasons for difference between experimental and numerical data such as leakage in the LAMEE, flow mal-distribution (Hemingson et al., 2011b) and heat loss (Seyed-Ahmadi et al., 2009a). The liquid desiccant leakage could be from the LAMEE to the environment or from a liquid channel to an air channel inside the LAMEE. The leakage from LAMEE to the environment would result in lower effectiveness values since Cr* would decrease. However, leakage from the desiccant channel to the air channel would cause higher effectiveness depending on the heat and moisture transfer direction. The numerical model does not include either leakage.

In addition, the numerical model assumes that there is a uniform desiccant distribution within the channels in the LAMEE, however, there could be a mal-distributed desiccant flow in the experiments, especially for low Cr* values - so the desiccant would not flow with a uniform speed between the membranes which would cause lower effectiveness values (Erb et al., 2009a). The heat losses from the LAMEE

sides are already considered in the numerical model, but there is also a potential for heat losses from liquid desiccant headers which are not considered in the numerical model.

Furthermore, the transient response of the LAMEE is studied under winter test conditions which the outdoor air is heated and humidified. The air inlet temperature and humidity ratio are T=7.8˚C and W=3.1 g/kg, respectively, while the solution inlet conditions are T_{sol}=26˚C and W_{sol}=13.3 g/kg. The numerical data are compared to the experimental data for NTU=8 and Cr*=3 and results are shown in Figure 3.8. As with the summer test conditions, the effectiveness increases with time and finally reaches a steady-state value. The numerical and experimental data show similar trends and values (e.g., the maximum difference between the measured and simulated effectiveness values is less than 10%), but it can be seen that there is a marked transition in the experimental data at about 5 minutes which does not exist in the numerical data. This transition is believed to be due to buoyancy forces within the liquid flow.

In winter operating conditions, when the warm desiccant enters the LAMEE from the bottom and is cooled by the membrane as it flows up, the buoyancy forces could cause a flow reversal where the cooler and denser desiccant near the membrane flow partly downward rather than continuously upward to the top of the exchanger. This phenomenon can reduce the exchanger performance in the winter operating conditions and this is likely one of the reasons for difference between numerical and experimental data at steady state and during the transient period for time greater than 5 minutes.

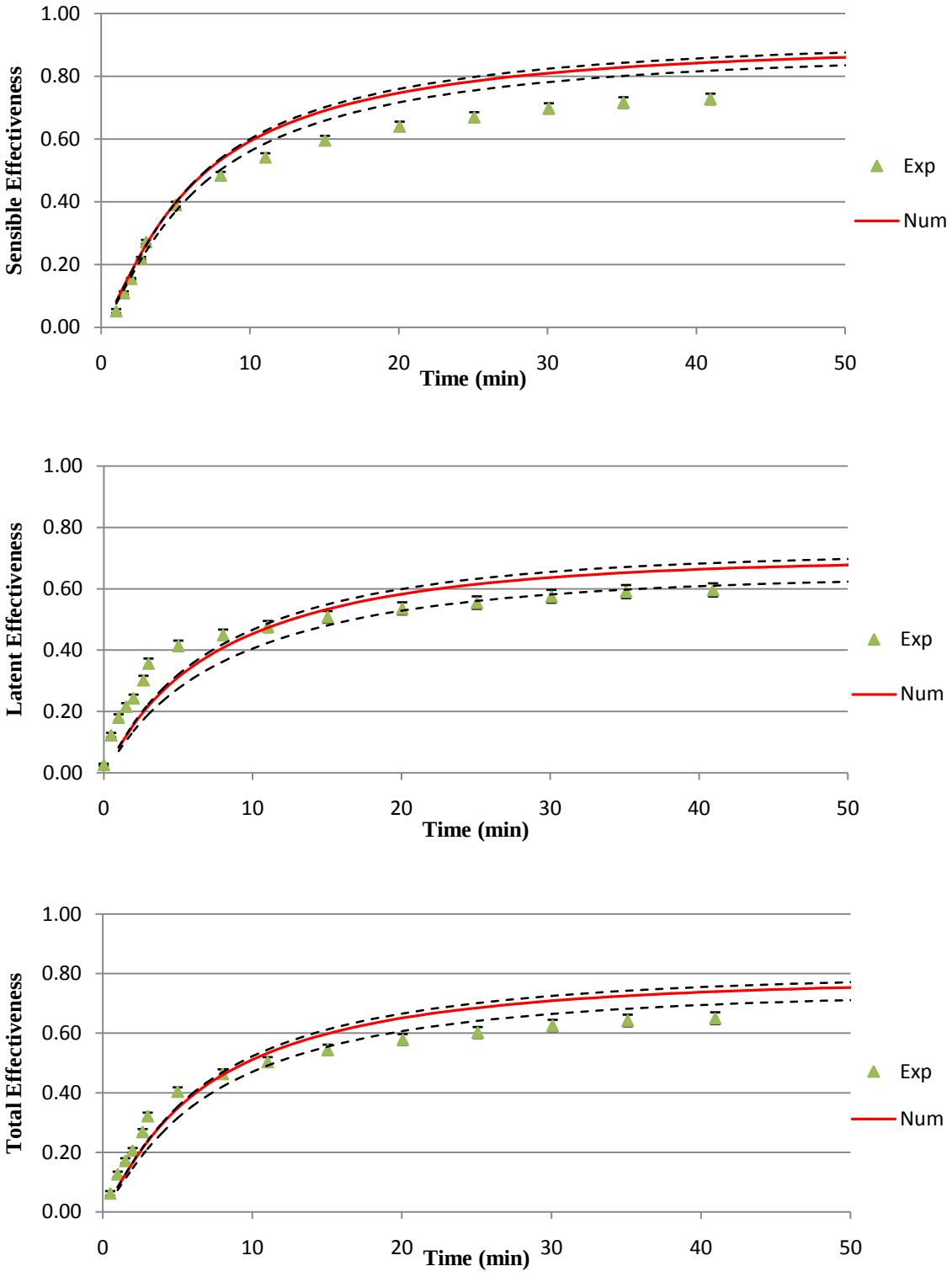

Figure 3.8 Transient sensible, latent and total effectiveness versus time for NTU=8 and Cr*=3 under winter test conditions ($T_{air,\,in}$= 7.8˚C, $W_{air,\,in}$=3.1 g/kg).

Figure 3.9 presents the Richardson and Grashof numbers in the liquid desiccant channel as a function of time for the winter test conditions. The results in Figure 3.9 show that both the space averaged Ri and Gr increase with time and finally reach a steady-state value. This figure implies that there may be significant a natural convection between the cold membrane and hot liquid as the Richardson number is much higher than 10. The Reynolds number for the liquid inside the channel is less than 1 and its value for each point is almost constant and there is only a slight difference due to kinematic viscosity variation as a result of temperature variation. However, Yao (1983) recommends that in isothermal vertical channels buoyancy effects can be neglected when Gr< Re, but as it is shown in this figure the range of Grashof number is 2-12 and is higher than Reynolds number during the test. Buoyancy forces appear to affect the LAMEE performance under winter test conditions. Further investigations are required to quantify how much the LAMEE performance is affected by buoyancy forces.

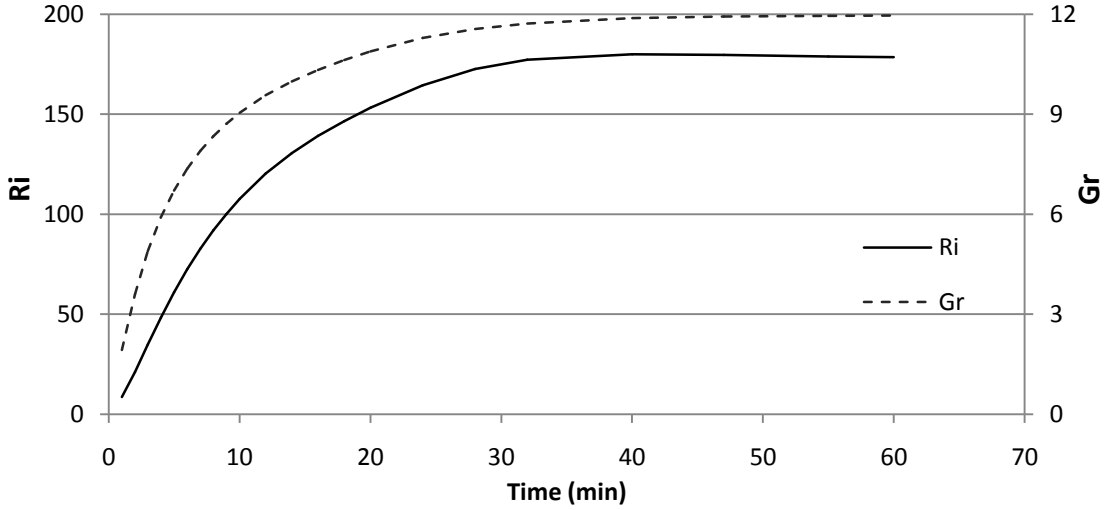

Figure 3.9 Transient Grashof and Richardson numbers under winter operating conditions.

3.7.1.2 Time Constant

The transient response of the LAMEE is investigated for different tests under summer test conditions. Time constant is used to characterize and compare the transient response of the LAMEE and it allows the effect of different parameters on the transient response to be compared conveniently. The air outlet temperature and humidity ratio as important transient parameters are characterized by an exponential correlation with two dimensionless weighting constants and two time constants (Namvar et al., 2012; Abe et al., 2006b):

$$\frac{\Delta\Phi}{\Delta\Phi_{\circ}} = X_1 e^{-t/t_1} + X_2 e^{-t/t_2} \tag{3.19}$$

where,

$\Delta\Phi = |\Phi - \Phi_i|$ change in variable φ (temperature or humidity ratio) at any time, t, compared to the initial value (φ_i)

$\Delta\Phi_{\circ} = |\Phi_f - \Phi_i|$ maximum change in the variable from its initial value to the final value

t_1, t_2 the first and second time constants

The weighting constants satisfy the equation:

$$X_1+X_2 = 1, \quad X_1 \geq 0, \quad X_2 \geq 0 \tag{3.20}$$

This correlation is fitted to the normalized air outlet temperature and humidity ratio and its coefficients, X_1, X_2, t_1 and t_2 are calculated for each test with different NTU and Cr* values. The first and second time constants correspond to the desiccant transport

time and thermal mass capacity of the LAMEE, respectively (Namvar et al., 2012). A single time constant is considered to compare results for different tests rather than these two time constants. This single time constant shows the time a transient variable has approached 63.2% of the difference between initial and final values:

$$\Phi_{\tau} = \Phi_{i} - 0.632\left|\Phi_{i} - \Phi_{f}\right| \tag{3.21}$$

According to this definition, the time constant is calculated for air outlet temperature and humidity ratio which correspond to the sensible and latent performance of the LAMEE, respectively. Experimental time constant values from (Namvar et al., 2012) are compared to numerical time constants to verify the model. Figure 3.10 shows the results for nine different tests with different air and desiccant mass flow rates under summer test conditions.

For a constant Cr*, both the experimental and numerical data show the time constant increases as NTU increases. As NTU increases, the air mass flow rate decreases and it takes longer for the LAMEE to reach to the steady-state conditions. For lower air mass flow rates, it takes longer the same mass of air passes the exchanger and same amount of energy be transferred between air flow and liquid desiccant. There is a very good agreement between experimental and numerical time constants for the humidity ratio or the LAMEE latent response, but agreement for the LAMEE thermal response is not good, especially for the lowest Cr*.

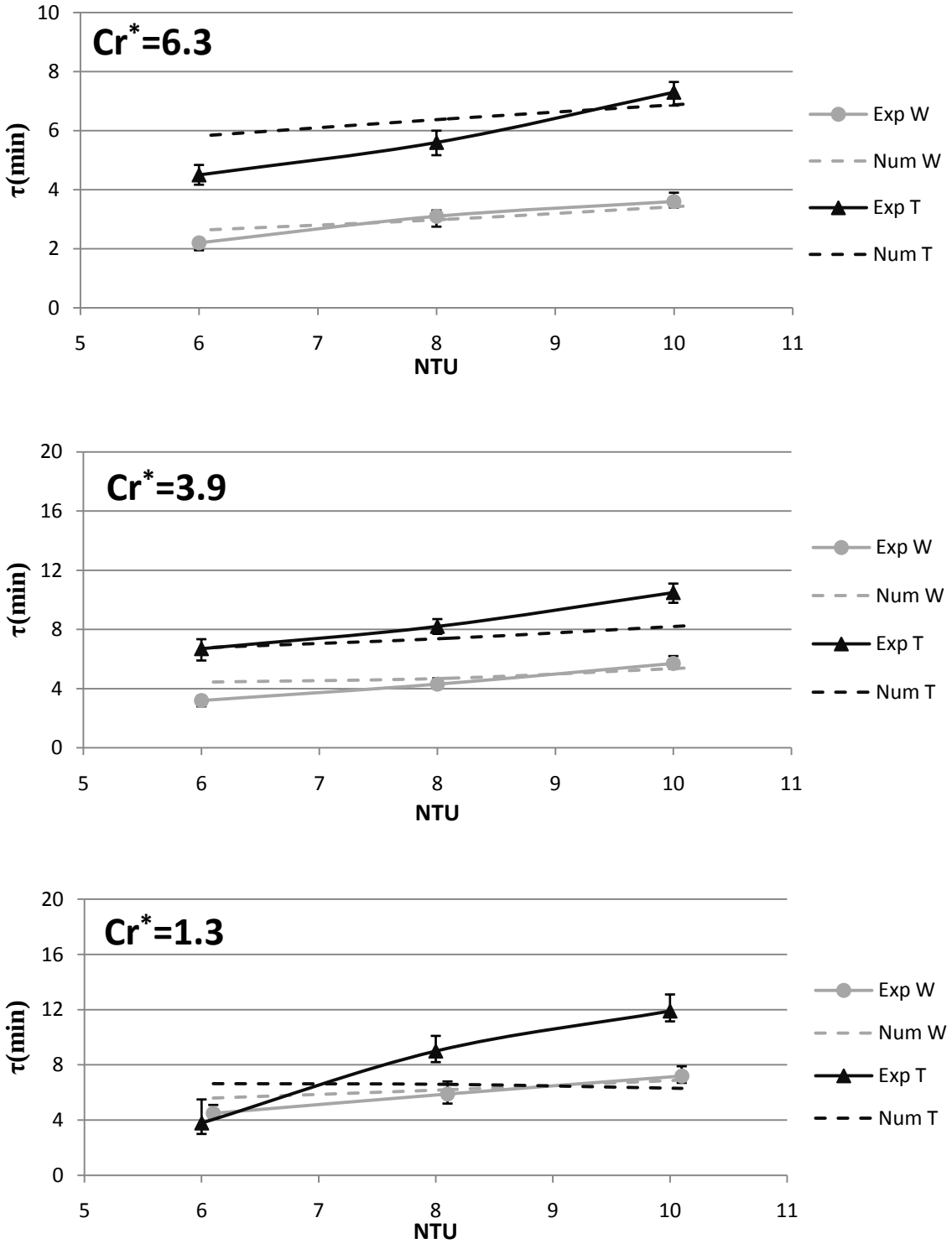

Figure 3.10 Numerical and experimental single time constants according to the air outlet conditions under summer operating conditions for Cr*=6.3, Cr*=3.9, and Cr*=1.3.

The verified numerical model is used to study the effect of outdoor air conditions on the transient response of the LAMEE. The time constant values are presented for various outdoor air conditions when the heat and moisture transfers between the air and liquid desiccant are in same direction (positive operating factor, +H*). In fact, the time constant is presented when the air is cooled and dehumidified or is heated and humidified. The liquid desiccant conditions are T_{sol} = 24˚C and W_{sol} = 9.3 g/kg and the NTU and Cr* values are 8 and 6.3, respectively. The initial conditions are assumed to be same as air inlet conditions. The results show that the sensible time constant does not change considerably with outdoor air conditions while the latent time constant is influences significantly by outdoor air conditions. As it is shown in Figure 3.11, the latent effectiveness decreases as H* increases, and approaches an asymptote at about τ = 4 min. But, the sensible time constant is almost independent of H*. For negative operating condition factors (-H*) which occur when heat and moisture are transferred in opposite directions, the time constant definition (equation (3.21)) is not applicable since the outdoor air humidity ratio variation does not exhibit an exponential decay. In some cases, the humidity ratio overshoots the final steady-state value.

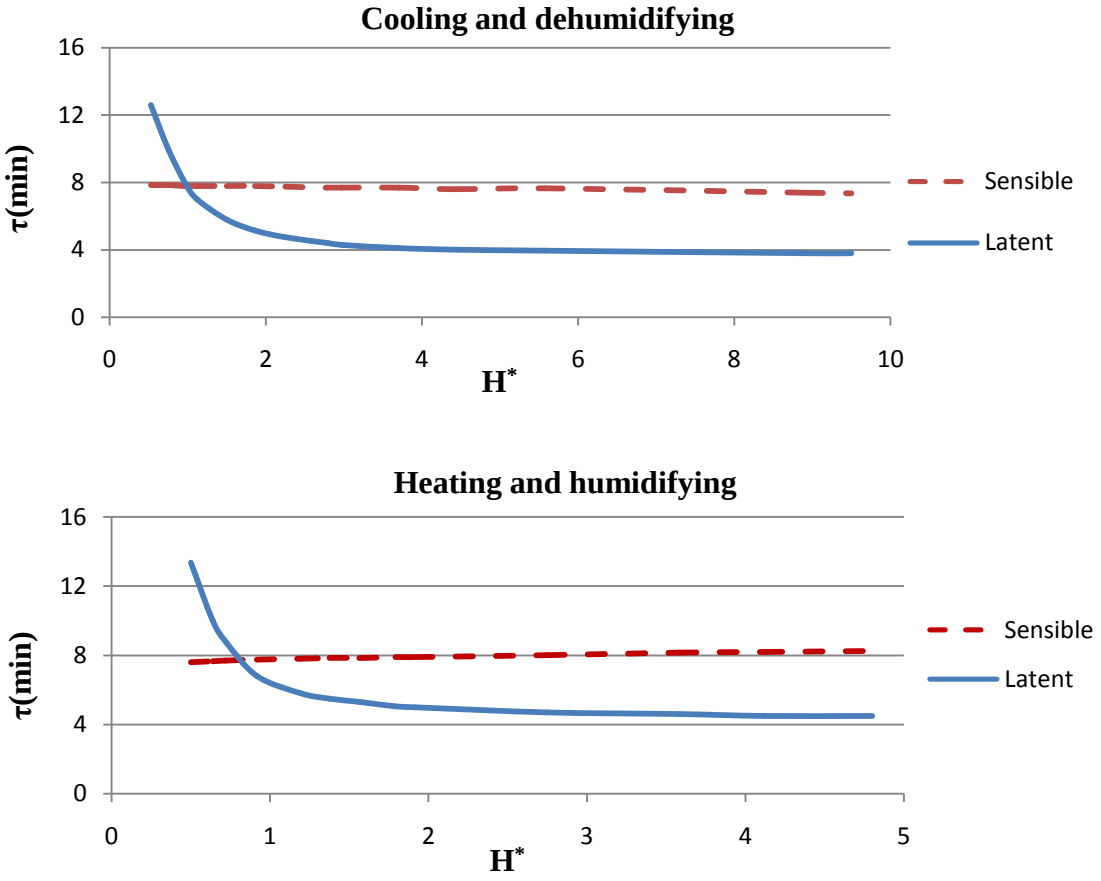

Figure 3.11 Sensible and latent time constants versus H* for cooling and dehumidifying, and heating and humidifying for NTU=8 and Cr*=6.3. The liquid desiccant inlet conditions are Tsol, in= 24˚C, Wsol, in= 9.3 g/kg.

3.8 Steady-State

3.8.1 Effect of Different Air and Liquid Desiccant Mass Flow Rates

The steady-state performance of the LAMEE under summer test conditions is studied in this research and the impact of the air and desiccant mass flow rates on the effectiveness is investigated. Figure 3.12 shows sensible, latent and total effectiveness for various tests with different NTU and Cr* values. The air and desiccant inlet conditions are kept almost same for all these experiments and the exact values are in Table 3.1. The average solution inlet conditions are T_{sol} = 24.4˚C and W_{sol} = 11.3 g/kg and the average air inlet conditions are T_{air} = 35˚C and W_{air} = 26 g/kg.

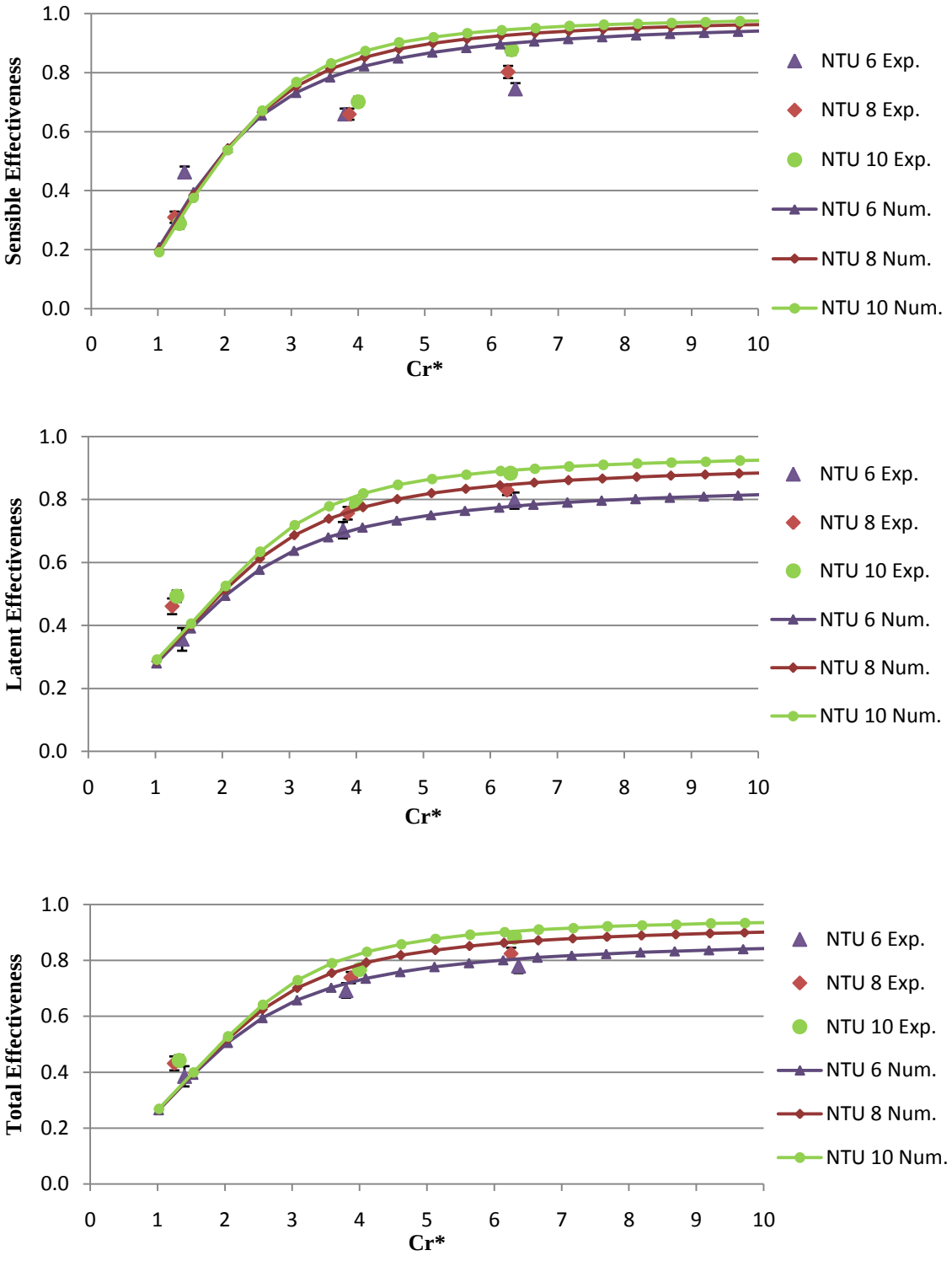

Figure 3.12 Steady-state sensible, latent and total effectiveness versus Cr* under summer operating conditions.

The numerical data are calculated for three different NTUs and Cr* between 1 and 10. As Cr* depends on both C_{sol} and C_{air}, the flow rate of the liquid desiccant is changed for each NTU to have a constant Cr*. Thus for a constant Cr*, a higher NTU means a lower desiccant mass flow rate. According to this figure, the sensible, latent and total effectiveness all increase as Cr* increases. In addition, the results show that as NTU increases, the effectiveness values increase; however, the latent effectiveness is more sensitive to changes in NTU than the sensible effectiveness under summer test conditions. Although the sensible effectiveness values are higher than latent ones, the total effectiveness trends and values are more similar to the latent effectiveness rather than sensible effectiveness. It means latent effectiveness is more dominant in the LAMEE under summer test condition.

The experimental results show that the effectiveness (sensible, latent and total) increases as Cr* increases for all NTU values which is confirmed by numerical results. Also, with a few exceptions, effectiveness increases as NTU increases. The latent and total effectiveness show good agreement between numerical and experimental data, but the sensible effectiveness agreement is not as good. Both numerical and experimental data show same response to Cr* variation. Both experimental and numerical results are more sensitive to Cr* in the range of 1 to 5, but they do not show much variation beyond that. According to Figure 3.12, the total effectiveness increases more than 40% when Cr* increases from 1 to 5 while it increases less than 10% when Cr* increases from 6 to 10.

3.8.2 Outdoor air conditions impact on the LAMEE performance

The verified numerical model is used to investigate the effect of outdoor air conditions on the LAMEE performance. The contour plots for the steady-state sensible and latent effectiveness of the LAMEE are presented on the psychometric chart. Each point on the psychometric chart presents the outdoor air conditions. The liquid desiccant conditions are T_{sol} = 24˚C and W_{sol} = 9.3 g/kg which correspond to AHRI summer indoor conditions (AHRI, 2005). The NTU and Cr* values are 8 and 6.3, respectively.

As it is shown in Figure 3.13a, the sensible effectiveness depends on outdoor air conditions. When outdoor air temperature is higher than inlet temperature of liquid desiccant (T>24˚C), the sensible effectiveness decreases as humidity ratio increases; however, for temperatures lower than liquid desiccant temperature (T<24˚C), the sensible effectiveness increases as humidity ratio increases. In summary, the sensible effectiveness decreases as H* increases.

The latent effectiveness depends also on the outdoor air conditions. According to Figure 3.13b, the latent effectiveness decreases with temperature increasing when the outdoor air humidity ratio is higher than liquid desiccant humidity ratio (W>9.3 g/kg), while the latent effectiveness increases as temperature increases when the outdoor air humidity ratio is less than liquid desiccant humidity ratio (W<9.3 g/kg). The latent effectiveness increases as H* increases (except when H* changes from $+\infty$ to $-\infty$ which occurs when the outdoor temperature is equal to the inlet liquid desiccant temperature, $T_{air}=T_{sol}$), and majority of outdoor air conditions show the latent effectiveness values between 70% and 85%.

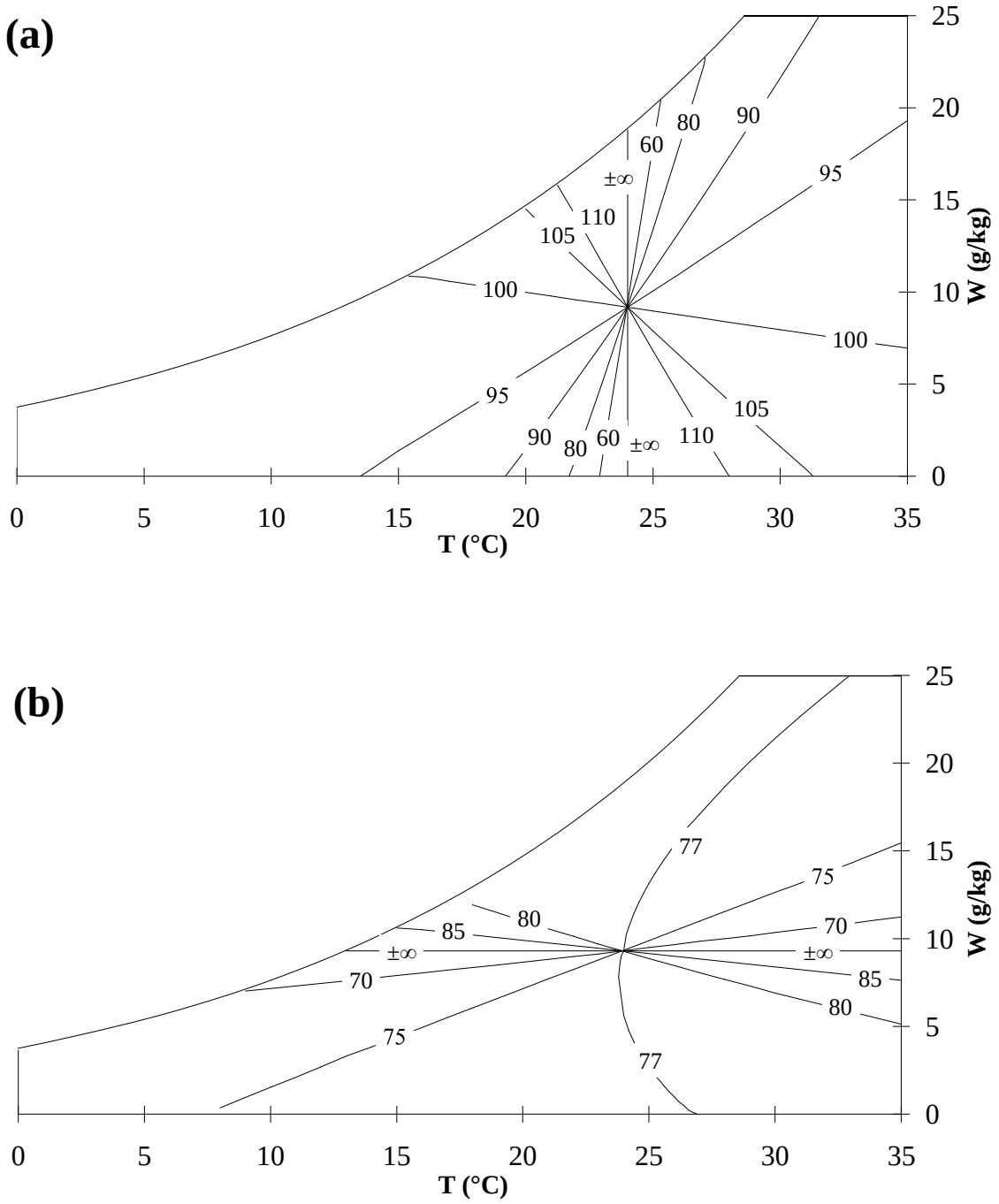

Figure 3.13 (a) Sensible effectiveness and (b) latent effectiveness of the LAMEE under various outdoor air conditions for NTU=8 and Cr*=6.3. The liquid desiccant inlet conditions are $T_{sol,\,in}$= 24˚C, $W_{sol,\,in}$= 9.3 g/kg.

The results reveal that the effectiveness response to the H* variation in the LAMEE is opposite to the RAMEE. For the RAMEE, the sensible effectiveness increases with H* increasing while the latent effectiveness decreases as H* increases (Hemingson et al., 2011a). For several outdoor air conditions, the effectiveness values are lower than 0% or higher than 100% due to low temperature difference or humidity ratio difference between the air and desiccant inlet conditions for sensible and latent effectiveness, respectively.

3.9 Conclusions

A liquid to air membrane energy exchanger (LAMEE) performance is investigated experimentally and numerically. Experimental data for a counter-cross LAMEE with Ay-tech ePTFE membranes under summer and winter test conditions are available in (Namvar et al., 2012). A numerical model is used to simulate the transient and steady-state performance of this LAMEE and the numerical results are compared to the published experimental data. In this model, the LAMEE thermal mass capacity, heat loss from sides and initial conditions are considered. The uncertainty of published experimental data (Namvar et al., 2012) due to uncertain initial conditions is clarified. The thermal mass of LAMEE panels and shell impact on the transient response of the LAMEE is quantified.

The transient response of the LAMEE is studied for different air and desiccant mass flow rates under summer and winter test conditions. There is an acceptable agreement between numerical and experimental data according to the RMSE and AAD values. In addition to the effectiveness, time constant is investigated as an important parameter in transient response of the LAMEE under summer tests conditions. Time

constants are determined according to the air outlet temperature and humidity which corresponde to the sensible and latent performance of the LAMEE, respectively. The numerical data are compared to the experimental data and the results show that time constant values increase as NTU increases or Cr* decreases. The numerical model is verified for transient effectiveness and time constant using experimental data. The numerical results show that the latent time constant is significantly affected by variation in the outdoor air conditions, while the sensible time constant does not depend on outdoor air conditions considerably.

In winter operating conditions, the buoyancy forces could affect the LAMEE performance. The results show that Grashof number is higher than Reynolds number under winter test conditions and buoyancy forces cannot be neglected. In addition, the Richardson number values are higher than 10 during transient period which shows the natural convection between the cold membrane and hot desiccant play an important role in the LAMEE performance.

The steady-state performance of the LAMEE is studied for different air and liquid desiccant mass flow rates under summer test conditions. For the latent and total effectiveness, there is very good agreement between experimental and numerical data while for the sensible effectiveness the differences between numerical and experimental data are up to 17%. Both numerical and experimental results show that the effectiveness values increase as either NTU or Cr* increase. The verified numerical model is used to investigate the effect of outdoor air conditions on LAMEE performance. The numerical data reveals that as H* increases the sensible effectiveness decreases, but the latent effectiveness increases.

CHAPTER 4

CONCLUSIONS

4.1 Conclusions

In this thesis, the performance of a counter-cross flow liquid-to-air membrane energy exchanger (LAMEE) is studied experimentally and numerically. The LAMEE is constructed from several semi-permeable membranes which allow heat and moisture transfer between the air and liquid desiccant streams without direct contact between these fluids. The liquid desiccant used in this research is $MgCl_2$ and the membrane is Ay-tech ePTFE.

The transient response of the LAMEE is investigated for different design and operating parameters (NTU, Cr*) under summer and winter test conditions. Both numerical and experimental results show that the sensible and latent effectiveness increase with time during transient period and finally reach a steady-state value. There is a good agreement between experimental and numerical results during both the transient and steady-state performance. It is found that there is a better agreement between numerical and experimental results for the latent effectiveness than for the sensible effectiveness. The average absolute difference (AAD) values for the sensible and latent effectiveness are 0.09 and 0.04, respectively. Also, the results reveal that total effectiveness values and trends are closer to the latent effectiveness rather than to

sensible effectiveness. In fact, moisture transfer plays a dominant role in the LAMEE performance for the test conditions study.

The LAMEE time constant is investigated under summer test conditions for different air and desiccant mass flow rates. The air outlet temperature and humidity ratio are normalized and curve-fitted with an exponential correlation with two dimensionless weighting factors and two time constants. The first time constant is less than 5 minutes for different NTU and Cr* values and correlates with the desiccant transport time in the exchanger, while the second time constant shows higher values (i.e., 5-24 min) and is correlated with the thermal mass capacity of the exchanger. In addition, a single time constant is defined to compare the transient response of the LAMEE for different NTU and Cr* values more conveniently. The single time constant shows the time that the transient variable (air outlet temperature or humidity ratio) reaches 63.2% of the difference between initial and final values of transient variable. Both numerical and experimental results show that the time constant increases as Cr* decreases or NTU increases. In other words, the LAMEE reaches steady-state conditions faster for higher air and desiccant mass flow rates. The LAMEE time constant is higher than the time constant of heat exchangers that transfer sensible heat only due to coupled heat and moisture transfer in the LAMEE and the large thermal and moisture capacities of the LAMEE. However, the single LAMEE responds faster than coupled LAMEEs or the RAMEE system.

The numerical model is verified with experimental data for both the transient and steady-state performance of the LAMEE. In this model, the LAMEE thermal mass capacity and heat loss from sides have been considered. The numerical model has been

used to study the impact of the air and desiccant initial conditions on transient response of the LAMEE and quantify the uncertainty of the experimental data due to uncertainties in the initial conditions. The verified numerical model is also used to investigate the effect of outdoor air conditions on the LAMEE time constant. It is found that the time constant is influenced by outdoor air conditions. The results reveal that the sensible time constant is not considerably sensitive to variation in the outdoor air conditions while the latent time constant is affected significantly by outdoor air conditions. The latent time constant decreases as H* increases when the heat and moisture transfer between the air and liquid desiccant are in same direction (positive H*).

Steady-state performance of the LAMEE is assessed for different air and desiccant mass flow rates under summer test conditions. Sensible, latent and total effectiveness are investigated experimentally, numerically and analytically for different NTU and Cr* values and the results reveal that the effectiveness increases as NTU or Cr* increases. The sensible effectiveness shows higher values than latent effectiveness, while the agreement between experimental and numerical results for the latent effectiveness is better than the sensible effectiveness. Also, the total effectiveness values and trends are again more similar to the latent effectiveness. Furthermore, the numerical results show that the steady-state sensible and latent effectivenesses of the LAMEE are influenced by the outdoor air conditions. The sensible effectiveness is more sensitive to outdoor air conditions and it is inversely proportional to H*. However, the latent effectiveness changes slightly for the majority of outdoor conditions. The latent effectiveness increases as H* increases.

4.2 Future Work

There are some additional topics that can be studied to optimize the design and improve the performance of a liquid-to-air membrane energy exchanger (LAMEE). Some of these topics are listed below:

- The solution mal-distribution impact on the LAMEE performance should be investigated experimentally and numerically with the aim to reduce mal-distribution effects in future LAMEE design. In the numerical model used in this thesis, the liquid desiccant flow is assumed to be uniform.
- The effect of outdoor air conditions on the LAMEE performance is presented numerically in this thesis. The results show that both the transient and steady-state effectiveness of LAMEE are influenced by outdoor air conditions. This phenomenon should be investigated experimentally as well.
- In this thesis, the transient response of the LAMEE is studied for a step change in desiccant inlet temperature. The effect of step change in air inlet temperature or air and desiccant mass flow rates could be investigated in future works.
- The application of the LAMEE in active HVAC systems could be studied in the future. In active systems, the desiccant solution inlet conditions are controlled to achieve the desired air outlet conditions.
- The transient and steady-state performance of the LAMEE depends on several parameters. In this research, the LAMEE performance is investigated experimentally and numerically, but an analytical solution could be developed to predict the heat and moisture characteristics in the LAMEE.

- For both experimental and numerical studies, $MgCl_2$ is used as a liquid desiccant. However, the performance of the LAMEE could be studied with different liquid desiccant.
- The LAMEE performance is influenced by buoyancy forces under specific operating conditions. Further experimental and numerical studies are necessary to characterize the buoyancy forces in the LAMEE and quantify their impacts on LAMEE performance.
- In this thesis, the LAMEE performance is investigated when the heat and moisture transfer occurs in same direction (heating and humidifying, cooling and dehumidifying). It would be worthwhile to study the LAMEE performance when the heat and moisture transfer are in opposite directions (heating and dehumidifying, cooling and humidifying).

REFERENCES

Abdelghani-Idrissi, M.A., Bagui, F., Estel, L., 2001. Analytical and experimental response time to flow rate step along a counter flow double pipe heat exchanger, *International Journal of Heat and Mass Transfer*, Vol. **44(19)** 3721-3730.

Abe, O.O., Simonson, C.J., Besant, R.W., Shang, W., 2006a. Effectiveness of energy wheels from transient measurements: Part I—Prediction of effectiveness and uncertainty, *International Journal of Heat and Mass Transfer* **(49)** 52–62.

Abe, O.O., Simonson, C.J., Besant, R.W., Shang, W., 2006b. Effectiveness of energy wheels from transient measurements: Part II— Results and verification, *International Journal of Heat and Mass Transfer* **(49)** 63–77.

Afshin, M., Simonson, C.J., Besant, R.W., 2010. Crystallization limits of LiCl-Water and MgCl2-Water salt solutions as operating liquid desiccant in the RAMEE system, *ASHRAE Transactions* **116(2)** 494-506.

AHRI, 2005. ANSI/ARI Standard 1060, Standard for Rating Air-to-Air Exchangers for Energy Recovery Ventilation Equipment. Arlington, VA: Air-Conditioning & Refrigeration Institute.

ANSI/ASHRAE Standard 55-2004, Thermal Environmental Conditions for Human Occupancy. Atlanta: ASHRAE.

ANSI/ASHRAE STANDARD 84-2008, Method of test for air-to-air heat/energy exchangers. American Society of Heating, Refrigerating, and Air-Conditioning Engineers, Atlanta.

ANSI/ASHRAE Standard 90.1-2007, Energy Standard for Buildings Except for Low-rise Residential Buildings, American Society of Heating, Refrigerating, and Air-Conditioning Engineers, Atlanta.

ASHRAE, ASHRAE Handbook-Fundamentals 2005, American Society of Heating, Refrigerating and Air-Conditioning Engineers, Inc., Atlanta, 2005.

ASME Performance Test Code 19.1-1998, Test Uncertainty: Instruments and Apparatus, New York, NY.

Ataer, O.E., Ileri, A., Gogus, Y.A., 1995. Transient behavior of finned-tube cross-flow heat exchangers, *International Journal of Refrigeration* **18 (3)**, 153–160.

Ataer, O.E., 2004. An approximate method for transient behavior of finned-tube cross-flow heat exchangers, *International Journal of Refrigeration* **27**, 529–539.

Bergero, S., Chiari, A., Isetti, C., 2001a. On the performance of a plane-plate membrane contactor for air dehumidification, *Proceedings of the 7th RHEVA World Congress Clima, Napoli.*

Bergero, S., Chiari, A., 2001b. Experimental and theoretical analysis of air humidification/ dehumidification processes using hydrophobic capillary contactors, *Applied Thermal Engineering* **21**, 1119-1135.

Bergero, S., Chiari, A., 2005. Enthalpy recovery in HVAC systems by means of membrane vapor exchangers and hygroscopic solution, *Proceedings of the 8th REHVA world congress Clima, Lausanne*.

Bergero, S., Chiari, A., 2010. Performance analysis of a liquid desiccant and membrane contractor hybrid air-conditioning system, *Energy and Buildings* **(42)** 11, 1976-1986.

Beriault, D., 2010. Run-around membrane energy exchanger prototype 4 design and laboratory, M.Sc. Thesis, University of Saskatchewan, Saskatoon, SK.

Bunce, D.J, Kandlikar, S.G., 1995. Transient response of heat exchangers, Heat and Mass Transfer 95, *Proceedings of the Second ISHMT-ASME Heat and Mass Transfer Conference*, Mangalore, India.

Charles, N.T., Johnson, D.W., 2008. The occurrence and characterization of fouling during membrane evaporative cooling, *Journal of Membrane Science* **319** 44–53.

Chiari, A., 2000. Air humidification with membrane contactors: experimental and theoretical results, *International Journal of Ambient Energy* **20 (4)**, 187-195.

Cisternas, L.A., Lam, E.J, 1991. An analytical correlation for the vapor pressure of aqueous and non-aqueous solutions of single and mixed electrolytes, Part II: Application and extension, *Fluid Phase Equilibrium* **62** 11–27.

Djongyang, N., Tchinda, R., Njomo, D., 2010. Thermal comfort: A review paper, *Renewable and Sustainable Energy Reviews* **14** 2626–2640.

Dwivedi, A.K., Das, S.K., 2007. Dynamics of plate heat exchangers subject to flow variations, *International Journal of Heat and Mass Transfer* **50**, 2733–2743.

Elenbaas, W., 1942. Heat dissipation of parallel plates by free convection, *Physica* 9, 1-28. Reprinted by Landis, F., 1986. W. Elenbaas' paper on Heat dissipation of parallel plates by free convection, *Heat Transfer in Electronic Equipment, ASME HTD*-Vol. **57**, 11-21.

Erb, B., Simonson, C.J., Seyed Ahmadi, M., Besant, R.W, 2009a. Experimental Measurements of a Run-Around Membrane Energy Exchanger (RAMEE) with Comparison to a Numerical Model, *ASHRAE Transactions*, **115(2)**.

Erb, B., 2009b. Run-around membrane energy exchanger performance and operational control strategies, M.Sc. Thesis, University of Saskatchewan, Saskatoon, SK.

Fan, H., Simonson, C.J., Besant, R.W., 2006. Performance of a run-around system for HVAC heat and moisture transfer applications using cross-flow plate exchangers coupled with aqueous lithium bromide, *HVAC R Res.* **12 (2)** 313–336.

Figliola, R.S., Beasley, D.E., 2000. Theory and Design for Mechanical Measurements, third ed., John Wiley & Sons, Inc.

Hemingson, H.B., Simonson, C.J., Besant, R.W., 2011a. Steady-state performance of a run-around membrane energy exchanger (RAMEE) for a range of outdoor air conditions, *International Journal of Heat and Mass Transfer* **54**, 1814–1824.

Hemingson, H.B., Simonson, C.J., Besant, R.W., 2011b.Effects of non-uniform channels on the performance of a run-around membrane energy exchanger (RAMEE), *Proceedings of the 12th International Conference on Air Distributions in Rooms (Roomvent 2011), Trondheim, Norway*.

Huang, S.M., Zhang, L.Z., Tang, K., Pei, L.X., 2012. Fluid flow and heat mass transfer in membrane parallel-plates channels used for liquid desiccant air dehumidification, *International Journal of Heat and Mass Transfer* **55**, 2571–2580.

Incropera, F.P., Dewitt, D.P., 2002. Fundamentals of Heat and Mass Transfer, fifth ed., John Wiley & Sons, New York.

Iskara, C., 2007. Convective mass transfer between a hydrodynamically developed airflow and liquid water with and without a vapor permeable membrane, M.Sc. Thesis, University of Saskatchewan, Saskatoon, SK.

ISO. 1991. ISO Standard 5167-1, Measurement of Fluid Flow by Means of Pressure Differential Devices. International Organization for Standardization.

Lachi, M., El Wakil, N., Padet, J., 1997. The time constant of double pipe and one pass shell-and-tube heat exchangers in the case of varying fluid flow rates, *International Journal of Heat and Mass Transfer*, Vol. **40 (9)** 2067–2079.

Larson, M.D., Simonson, C.J., Besant, R.W, Gibson, P.W., 2007. The elastic and moisture transfer properties of polyethylene and polypropylene membranes for use in liquid-to-air energy exchangers, *Journal of Membrane Science* **302** 136–149.

Mahmud, K., 2009. Design and performance of counter-cross flow run-around membrane energy exchanger system, M.Sc. Thesis, University of Saskatchewan, Saskatoon, SK.

Mahmud, K., Mahmood, G.I., Simonson, C.J., Besant, R.W., 2010. Performance testing of a counter-cross-flow run-around membrane energy exchanger (RAMEE) system for HVAC applications, *Energy and Buildings* **42**, 1139-1147.

Min, J., Su, M., 2010a. Performance analysis of a membrane-based enthalpy exchanger: Effects of the membrane properties on the exchanger performance, *Journal of Membrane Science* **348**, 376–382.

Min, J., Su, M., 2010b. Performance analysis of a membrane-based energy recovery ventilator: Effects of membrane spacing and thickness on the ventilator performance, *Applied Thermal Engineering* **30**, 991–997.

Namvar, R., Pyra, D., Ge, G., Simonson, C.J., Besant, R.W., 2012, Transient characteristics of a liquid-to-air membrane energy exchanger (LAMEE) experimental data with correlations, accepted in *The International Journal of Heat and Mass Transfer*.

Nasif, M.S., Morrison, G.L. Behnia, M., 2005. Heat and mass transfer in air to air enthalpy heat exchangers, *6th World Conference on Experimental Heat Transfer, Fluid Mechanics and Thermodynamics, Matsushima, Miyagi, Japan*.

Niu, J.L., Zhang, L.Z., 2001. Membrane-based Enthalpy Exchanger: material considerations and clarification of moisture resistance, *Journal of Membrane Science* **189**, 179–191.

Perez-Lombard, L., Ortiz, J., Pout, C., 1998. A review on buildings energy consumption information, *Energy & Buildings* **40(3)** 394-8.

Rasouli, M., Simonson, C.J., Besant, R.W., 2010a. Applicability and optimum control strategy of energy recovery ventilators in different climatic conditions, *Energy and Buildings* **42(9)**, 1376-1385.

Rasouli, M., Simonson, C.J., Besant, R.W., 2010b. Energetic, economic and environmental analysis of a health-care facility HVAC system equipped with a run-around membrane energy exchanger, submitted to *Journal of Energy and Buildings.*

Rasouli, M., Simonson, C.J., Besant, R.W., 2010c. Optimization of energy recovery ventilators and their impact on energy and comfort, *submitted to Journal of Energy.*

Seyed-Ahmadi, M., Erb, B., Simonson, C.J., Besant, R.W. 2008a. Modeling and Simulation of the Transient Behavior of Run-around Heat and Moisture Exchanger System, Part I: Model Formulation and Verification, *International Journal of Heat and Mass Transfer* **52**(25-26), 6000-6011.

Seyed-Ahmadi, M., Erb, B., Simonson, C., Besant, R.W. 2008b. Modeling and Simulation of the Transient Behavior of Run-around Heat and Moisture

Exchanger System, Part II: Sensitivity Studies for a Range of Initial conditions, *International Journal of Heat and Mass Transfer* **52**(25-26), 6012-6020.

Seyed-Ahmadi, M., 2008c. Modeling the Transient Behavior of a Run-around Heat and Moisture Exchanger System, M.Sc. Thesis, University of Saskatchewan, Saskatoon, SK.

Shah, R.K, 1981, The transient response of heat exchangers, in: S. Kalpak, A.E. Bergles, F.Mayinger (Eds.), Heat Exchangers, Thermal-Hydraulic Fundamentals and Design,Hemisphere Publishing Co, Washington, 1981, 915–954.

Simonson, C.J., Besant, R.W., 1999. Energy wheel effectiveness: Part I-Development of dimensionless groups, *International Journal of Heat and Mass Transfer*, **42**, 2161-2170.

Spiga, M., Spiga, G., 1988. Transient temperature fields in crossflow heat exchangers with finite wall capacitance, *Journal of heat transfer* **110 (1)**, 49–53.

Spiga, M., Spiga, G., 1992. Step response of the cross-flow heat exchanger with finite wall capacitance, *International Journal of Heat and Mass Transfer* **35 (2)**, 559–565.

Srihari, N., Prabhakara Rao, B., Sunden, B., Das, S. K., 2005. Transient response of plate heat exchangers considering effect of flow maldistribution, *International Journal of Heat and Mass Transfer* **48**, 3231–3243.

Srihari, N., Das, S. K., 2008. Experimental and theoretical analysis of transient response of plate heat exchangers in presence of nonuniform flow distribution, *Journal of Heat Transfer,* Vol. **130**.

Teertstra, P., Culham, J.R, Yovanovich, M.M, 1997. Comprehensive review of natural and mixed convection heat transfer models for circuit board arrays, *Journal of Electronics Manufacturing,* Vol**. 7 (2)** 79-92.

Vaisi, A., Talebi, S., Esmaeilpour, M., 2011. Transient behavior simulation of fin-and-tube heat exchangers for the variation of the inlet temperatures of both fluids, *International Journal of Heat and Mass Transfer* **38**, 951–957.

Vali, A., 2009. Modeling a Run-around Heat and Moisture Exchanger System Using Two Counter/Cross Flow Exchangers, M.Sc. Thesis, University of Saskatchewan, Saskatoon, SK.

Wang, Y.H., Besant, R.W., Simonson, C.J., Shang, W., 2006. Application of humidity sensors and an interactive device, *Sensors and Actuators B Chemical **115 (1)***, 93–101.

Yao, L. S., 1983. Free and forced convection in the entry region of a heated vertical channel, *International Journal of Heat and Mass Transfer* **26**, 65-72.

Yin, J., Jensen, M.K., 2003. Analytic model for transient heat exchanger response, *International Journal of Heat and Mass Transfer* **46**, 3255–3264.

Zhang, L.Z., Jiang, Y., 1999. Heat and mass transfer in a membrane-based energy recovery ventilator, *Journal of Membrane Science* **163**, 29-38.

Zhang, L.Z., 2011. An analytical solution to heat and mass transfer in hollow fiber membrane contactors for liquid desiccant air dehumidification, *Journal of Heat Transfer* **133 (9).**

Zhang, L.Z., Huang, S.M., Chi, J.H., Pei, L.X., 2012. Conjugate heat and mass transfer in a hollow fiber membrane module for liquid desiccant air dehumidification: A free surface model approach, *International Journal of Heat and Mass Transfer* **55**, 3789–3799.

APPENDIX A

COPYRIGHT PERMISSIONS

This Appendix includes the copyright permission from the publisher of manuscript #1 and co-authors who contributed in manuscript # 2.

A.1. Manuscript #1

For previously published manuscripts that form a part of a thesis, written permission from the publisher (copyright holder) is required by the College of Graduate Studies and Research (CGSR). For manuscripts published by Elsevier, the authors retain the right to include their publication in a thesis without requesting a written permission:

"*As an author, you retain rights for a large number of author uses, including use by your employing institute or company. These rights are retained and permitted without the need to obtain specific permission from Elsevier. These include: the right to include the article in full or in part in a thesis or dissertation (provided that this is not to be published commercially); the right to use the article or any part there of in a printed compilation of works of the author, such as collected writings or lecture notes (subsequent to publication of the article in the journal); and the right to prepare other derivative works, to extend the article into book-length form, or to otherwise re-use portions or excerpts in other works, with full acknowledgement of its original publication in the journal*."

This information is available at the publisher's website at: http://support.elsevier.com/app/answers/detail/a_id/565/session/L3RpbWUv , Sep. 11, 2012.

A.2. Manuscript #2

For unpublished manuscripts, written permission from co-authors is required by CGSR to include the manuscript in a thesis.

Copyright Permission Request Form

I am preparing the publication of manuscript titled:

Transient heat and moisture transfer characteristics of a liquid-to-air membrane energy exchanger (LAMEE) model verification and extrapolation

to be published as the third chapter of my M.Sc. thesis, and to be submitted to the Department of Mechanical Engineering at the University of Saskatchewan. The authors contributing in the completion of this manuscript are as follows:

Ramin Namvar, Carey J. Simonson[*]*, Robert W. Besant*

I am requesting permission to use the materials described in aforementioned manuscript in my M.Sc. thesis and all subsequent editions that may be prepared at the University of Saskatchewan. Please indicate agreement by signing below:

Yours sincerely,
Ramin Namvar
Sep. 11, 2012

Permission granted by:

Signature:

Date:

Copyright Permission Request Form

I am preparing the publication of manuscript titled:

Transient heat and moisture transfer characteristics of a liquid-to-air membrane energy exchanger (LAMEE) model verification and extrapolation

to be published as the third chapter of my M.Sc. thesis, and to be submitted to the Department of Mechanical Engineering at the University of Saskatchewan. The authors contributing in the completion of this manuscript are as follows:

Ramin Namvar, Carey J. Simonson[*]*, Robert W. Besant*

I am requesting permission to use the materials described in aforementioned manuscript in my M.Sc. thesis and all subsequent editions that may be prepared at the University of Saskatchewan. Please indicate agreement by signing below:

Yours sincerely,
Ramin Namvar
Sep. 11, 2012

Permission granted by:

Signature:

Date: